Article type: Review

Evolution of Bioengineered Lung Models: Recent Advances and Challenges in Tissue Mimicry for Studying the Role of Mechanical Forces in Cell Biology

Ali Doryab, *Sinem Tas*, *Mehmet Berat Taskin, Lin Yang, Anne Hilgendorff*, *Juergen Groll*, *Darcy E. Wagner*, *Otmar Schmid**

A. Doryab
Comprehensive Pneumology Center Munich (CPC-M), Member of the German Center for Lung Research (DZL), 81377, Munich, Germany

Institute of Lung Biology and Disease (iLBD), Helmholtz Zentrum München—German Research Center for Environmental Health, 85764, Neuherberg, Germany

Munich Medical Research School (MMRS), Faculty of Medicine, Ludwig-Maximilians-University of Munich (LMU), 80336, Munich, Germany

Dr. S. Tas, Dr. D. E. Wagner
Department of Experimental Medical Sciences, Lung Bioengineering and Regeneration, Lund University, 22100, Lund, Sweden

Stem Cell Centre, Lund University, 22184, Lund, Sweden

Wallenberg Center for Molecular Medicine, Lund University, 22100, Lund, Sweden

Dr. M.B. Taskin, Prof. J. Groll
Department of Functional Materials in Medicine and Dentistry and Bavarian Polymer Institute (BPI), University of Würzburg, 97070, Würzburg, Germany

Dr. A. Hilgendorff
Comprehensive Pneumology Center (CPC-M), University Hospital of the University of Munich and Helmholtz Zentrum Muenchen, 81377, Munich, Germany.

Department of Neonatology, Perinatal Center Grosshadern, Ludwig-Maximilians University, 80337, Munich, Germany.

Center for Comprehensive Developmental Care, Dr. von Haunersches Children's Hospital University, Hospital Ludwig-Maximilians University, 81377, Munich, Germany.

L. Yang, Dr. O. Schmid*
Comprehensive Pneumology Center Munich (CPC-M), Member of the German Center for Lung Research (DZL), 81377, Munich, Germany

Institute of Lung Biology and Disease (iLBD), Helmholtz Zentrum München—German Research Center for Environmental Health, 85764, Neuherberg, Germany

E-mail: otmar.schmid@helmholtz-muenchen.de

Abstract

Mechanical stretch under both physiologic (breathing) and pathophysiologic (ventilator-induced) conditions is known to significantly impact all cellular compartments in the lung thereby playing a pivotal role in lung growth, regeneration and disease development. In order to sensitively and specifically evaluate the consequences exerted by mechanical forces on the cellular level, *in vitro* models using lung cells on stretchable membranes have been developed. Only recently have some of these cell-stretching devices become suitable for air-liquid interface cell cultures, which is required to adequately model physiologic conditions for the alveolar epithelium. To reach this goal, a membrane for cell growth balancing biophysical and mechanical properties is critical to mimic (patho)physiologic conditions. In this review, we i) provide insight into the relevance of cyclic mechanical forces in lung biology, ii) describe the physiologic range for the key parameters of tissue stretch in the lung and iii) discuss the currently available *in vitro* cell-stretching devices. After assessing various polymers, we conclude that natural-synthetic copolymers are promising candidates for suitable stretchable membranes used in cell-stretching models. This article will provide guidance on future developments in biomimetic *in vitro* models of the lung with the potential to function as a template for other organ models (e.g. skin and vessels).

Keywords: tunable polymeric membrane, porous ultra-thin scaffold, alveolar-capillary barrier, air-liquid interface cell culture*, in vitro* cell-stretching model

Abbreviations

1HAEo- and 16HBE14o-: Airway epithelial cells
3D: Three-dimensional
A549: Immortalized human alveolar epithelial cell line: A549
ADSCs: Human adipose-derived stem cells
ALI: Air-liquid interface
ARDS: Acute respiratory distress syndrome
ASMs: Airway smooth muscle cells
ATs: Alveolar epithelial cells
ATIs: Type I alveolar epithelial cells
ATIIs: Type II alveolar epithelial cells
BASMCs: Bovine aortic smooth muscle cell
cAMP: Cyclic adenosine 3′,5′-monophosphate
COPD: Chronic obstructive pulmonary disease
DCs: Dendritic cells
dECM: Decellularized extracellular matrix
DMSO: Dimethylsulfoxide
ECM: Extracellular matrix
EGF: Epidermal growth factor
EGFR: Epidermal growth factor receptor
EMT: Mesenchymal transition
ERK: Extracellular-regulated protein kinase
ES: Electrospinning
EVs: Extracellular vesicles
FAK: Focal adhesion kinase
FEK4: Human skin primary fibroblast cells
GAPDH: Glyceraldehyde 3-phosphate dehydrogenase
HBSMCs: Human bronchial smooth muscle cells
HFIP: 1,1,1,3,3,3-Fluoro-2-propanol
HFP: Hexafluoro-2-propanol
HIF-1α: Hypoxia-inducible factor 1α
HLEC: Human limbal epithelial cell
HPAEC: Primary human pulmonary alveolar epithelial cells
HPMEC: Primary human pulmonary microvascular endothelial cell
HSAEC: Primary human small airway epithelial cells
HUSMCs: Human umbilical arterial smooth muscle cells
HUVECs: Human umbilical vein endothelial cells
iCVD: Initiated chemical vapor deposition
IKVAV: Isoleucine-lysine-valine-alanine-valine
IL-8: Interleukin-8
IPF: Pulmonary fibrosis
LSFM: Light sheet fluorescence microscopy
MALI: Moving Air Liquid Interface
MAPK: Mitogen-activated protein kinases
mATII: Mouse alveolar epithelial type II cells
MLE-12: Mouse lung epithelial cells
NCI H44: Human lung carcinoma epithelial cell line
NCI-H441: Human pulmonary epithelial cell line
NCO–sP(EO-stat-PO): Star-shaped poly(ethylene oxide-stat-propylene oxide) with isocyanate end groups
NOF: Normal oral fibroblasts

NOK: Normal oral keratinocytes
OSA: Obstructive sleep apnea
P(LLA-CL): Poly(l-lactide-co-caprolactone)
PCL: Poly(ε-caprolactone)
PCLS: Precision-cut lung slices
PCU: Polycarbonate polyurethane
PDMS: Poly(dimethylsiloxane)
PDS: Polydioxanone
PEECs: Porcine esophageal Epithelial cells
PEGdma: Poly(ethylene glycol) dimethacrylate
PET: Polyethylene terephthalate
PGA: Polyglutamic acid, HA: hyaluronan
PGS: Poly(glycerol sebacate)
pHPAEC: Primary human pulmonary alveolar epithelial cells
PKA: Protein kinase A
PLA: Polylactic acid
PLGA: Poly(lactic-co-glycolic acid)
PLLA: Poly-L-lactic acid
PTFE: Poly(tetrafluoroethylene)
PVA: Poly(vinyl alcohol)
rATII: Rat alveolar epithelial type II cells
RGD: Arginylglycylaspartic acid
rhTE: Recombinant human tropoelastin
rMSCs: Rat mesenchymal stem cells
SMCs: Smooth muscle cells
SP-B: Surfactant protein B
SP-C: Surfactant protein C
TACE: Tumor Necrosis Factor-alpha-converting Enzyme
TAZ: Transcriptional co-activator with PDZ-binding motif
TEER: Transepithelial electrical resistance
TFE: Trifluoroethanol
VECs: Valvular endothelial cells
VICs: Valvular interstitial cells
VILI: Ventilator-induced lung injury
YAP: Yes-associated protein

1. Introduction

Respiratory diseases such as chronic obstructive pulmonary disease (COPD) and asthma are among the leading causes of death worldwide and will be the third leading cause of death by 2020. In the US alone it is estimated that the direct and indirect healthcare expenditure of COPD will be $50 billion [1]. In spite of the expected increase in prevalence of chronic lung disease, there are currently no cures – only symptomatic therapies and lung transplantation for end-stage disease patients [2,3].

The lung gains its most critical and sophisticated functionality through the defined arrangement of an extracellular matrix (ECM) which is maintained and populated by a variety of ca. 60 different cell types. All of the different cellular compartments in the lung face a continuous but dynamic environment due to mechanical forces occurring with each breath. The main pulmonary function of gas exchange at the epithelial-endothelial interface goes hand in hand with the surveillance of complex environment-host interactions. Although these critical functions are enabled by the presence and interaction of various cell types, direct exposure to gases and airborne particles, including cigarette smoking, combustion/industrial/occupational emissions or inadvertently released (nano-)particles from consumer products is known to put the lungs at risk for environmentally induced diseases outlined above [4].

In light of the urgent need for further research into the mechanisms of lung disease and novel therapeutic concepts, experimental approaches have largely utilized animal models or isolated primary cells [5,6]. Despite sophisticated effort in this research field, translation of promising drug candidates from animal, mostly rodent, models into the clinical setting often fails. In order to meet this need, an increasing number of biomimetic *in vitro* and *ex vivo* lung tissue models have been developed to i) study specific cellular effects and ii) translate observations into the clinic.

Efforts toward more biomimetic *in vitro* cell models include multi-cell co-culture models consisting of up to five different cell types and the shift from cell lines to potentially more physiologic primary cell cultures, which includes the most recent lung-on-a-chip technology [7]. In recent years, these efforts also started to recognize the role of mechanical stimuli, that not only play a role in lung development and regeneration, but when pathologic, have also been shown to have a role in disease onset, mitigation and chronicity [8,9]. Mechanical stretch has been shown to modify cell proliferation, differentiation, secretion, and migration through regulation of specific signaling pathways leading to changes in gene expression and protein synthesis [10,11]. **Figure 1** depicts an overview over the most relevant mechanisms induced or impacted by a cellular stretch. Despite acknowledging of the importance of mechanical forces to mimic (patho)physiologic conditions (and thus reliably study relevant treatment and injury mechanisms), only a very limited number of *in vitro* models allow mechanical stretching of pulmonary epithelial cells. Moreover, nearly all of these models were designed for non-physiologic submerged conditions with cell culture medium completely covering the cells, rather than physiologic air-liquid interface (ALI) culture conditions (**Figure 2**a), where epithelial cells are exposed to air resulting in cell polarization and secretion of a protective liquid layer such as mucus and/or alveolar lining fluid [10,12–16]. This was mainly owed to establishing feasibility, i.e. the technological simplicity of submerged cell culture systems. Only a few of these cell-stretching devices are commercially available (e.g. Bioflex® culture plate, Flexcell International Corp., USA) and thus there has been a challenge of bringing these setups to biologists with expertise in pulmonary biology (Figure 2e). On the other hand, the advantages of cell and tissue-based bioreactor systems includes the creation of biomimetic culture conditions that significantly improve the physiological relevance of cell and tissue cultures by controlling microenvironment parameters and facilitating mass transfer of

nutrients [17–20]. Nonetheless, one of the main limitations of the currently available stretchable systems is the lack of suitable membranes which are both suitable for ALI cell culture conditions and closely mimicking the physiologic conditions in the lung.

In order to address these questions, the present review focuses on *in vitro* devices for cyclic stretch as well as ALI culture conditions of pulmonary epithelial cells, which have been developed in the past decade (Figure 2b). The technical aspects of these systems are presented and the physiologic implications of stretch on cellular function and biological response as well as membrane design, candidate materials, and manufacturing processes are reviewed. Furthermore, the potential of alternative membrane materials for improved biomimetic characteristics are discussed.

2. Stretch-related lung biology

Lung has a complex architecture partitioned into 23 generations of airways enabling oxygen transport and carbon dioxide transport in and out of the blood, respectively, via the large air-liquid interface presented by the surface area of the alveolar tissue (gas exchange region of the lung) [21]. **Figure 3**a depicts the whole murine lung from trachea, bronchus, bronchioles (I-II) down to the typical three-dimensional honeycomb architecture of the alveoli (III-V). The surface of the lung is covered with epithelial cells, which represent the interface between air and liquid (tissue) typically referred to as ALI. Strictly speaking, the entire epithelium is not directly exposed to air, since epithelial cells secrete a protective liquid layer consisting of mucus and/or alveolar lining fluid in the bronchial and alveolar region, respectively. These conditions can be mimicked *in vitro* by air-lifting epithelial cells and exposing them to air (ALI culture). The alveolar region is an elastic and mechanically dynamic part of the lung experiencing nearly constant cyclic stretch motion with significant impact on many aspects of lung metabolism, function, and growth [22,23]. The

mechanical forces are mainly a result from inspiratory inflation and expiatory deflation of the lung and to a lesser degree due to pulsatile blood flow.

2.1. Physiologic stretch and biological membrane conditions

During normal tidal breathing at rest (ca. 500 mL tidal volume), a healthy lung normally inflates at a frequency of ca. 0.20 Hz (12-15 inhalation-exhalation cycles per minute for rest conditions) causing the alveoli to increase in size and surface area (**Table 1**). Under these respiratory conditions, the basement membrane, which represents the structural core of the air-blood barrier, is stretched to a linear strain of 4% [24–26]. During heavy exercise the respiratory frequency and tidal volume can increase up to about 0.55 Hz (26-33 breaths per minute) and 1900 mL, respectively [27], resulting in an increase in linear strain of ca. 12% in the alveoli [28] reaching even 20% in pathological scenarios such as acute respiratory distress syndrome (ARDS)[29].

A thin basement membrane (thickness ca. 50 nm) lies underneath both the epithelial and endothelial cell layers and consists of small fibrils of collagen and elastin and rare fibroblasts (Figure 3a-c). In the alveolar-capillary barrier these two basal laminae are fused so that no interstitial tissue can form between them [30]. These basement membranes are a permeable barrier with diminutive tiny pores. Although there is no general opinion about the size of these pores, some reports on animal lungs [31,32] suggest two types of pores one being <2.5 nm in diameter and a small fraction of larger pores (<400 nm) [33]. The mean thickness of the alveolar-capillary barrier (region of fused epithelial-endothelial basement membrane) is 1.1 μm [30,34]. The average thickness of the air-blood barrier (alveolar-capillary barrier at the site of gas exchange) is smaller (0.62 μm) [30,35], since the gas exchanges occurs preferentially at the sites of closest proximity between air and blood. The stiffness of healthy whole human alveolar tissue (measured as Young's elastic modulus) is estimated to range between 1-2 kPa [36,37]. Under pathological conditions such as

idiopathic pulmonary fibrosis (IPF), the stiffness of the basement membrane can increase to ca. 16.5 kPa [37] due to enhanced secretion and deposition of ECM proteins by both epithelial cells and fibroblasts.

2.2. Role of mechanical stretch in lung biology

Mechanoreceptors on the cell surface can detect mechanical stretch and subsequently convert this stimulation into biochemical signals activating downstream signaling pathways [38]. The consequences of mechanical forces on lung biology has been determined from numerous *in vivo* and *in vitro* experiments and is summarized in Figure 1. **Table 2** presents an overview of the results from *in vitro* studies covering a wide range of stretch conditions and cell types.

Cyclic mechanical stretch has been shown to alter proliferation, differentiation, and migration of pulmonary epithelial cells [10,11,39–44]. These effects can be mediated by activation of several distinct cellular pathways such as the mitogen-activated protein kinase /extracellular-regulated protein kinase (MAPK/ERK) pathway via binding of the epidermal growth factor (EGF) to the epidermal growth factor receptor (EGFR), which results in the differentiation of fetal epithelial cells [45]. Fetal alveolar epithelial type II cells (ATIIs) can be induced via activation of the transcription factor-dependent protein kinase (cAMP-PKA-dependent) signaling pathway during cyclic equibiaxial elongation [46]. It has also been shown that YAP (Yes-associated protein) is a key mediator in regulating cyclic mechanical stretch and together with the signaling cascade (the Cdc42/F-actin/MAPK), they can promote alveolar regeneration [47]. YAP and TAZ (Transcriptional co-activator with PDZ-binding motif), the Hippo signal-regulated transcriptional co-activators, can also be stimulated by the mechanical signals that are sensed by cells and trigger cell survival signaling [48]. In addition, cyclic stretch can alter cell morphology of alveolar epithelial cells (ATs) and activate Src protein tyrosine kinase [49] including actin cytoskeleton remodeling and cell alignment (and orientation) in fetal ATIIs and can be regulated via RhoA and

Rac1 signaling proteins, members of the Rho small GTPase family of hydrolyzing enzymes, when cells experience mechanical stretch [50].

Studying the effects of mechanical distension on the expression of specific markers for the alveolar epithelial type I (ATI) and type II (ATII) cell phenotypes showed that mechanical distension (21%, surface area) influences alveolar epithelial phenotypic expression *in vitro* at the transcriptional level and it appears that both transcriptional and posttranscriptional mechanisms are involved [51]. Mechanical stretch can influence the expression of ECM components [52], proliferation rate [10] and may also impact the expression of surfactant protein C and B (SP-C and SP-B) [53–56], synthesis of surfactant-related phospholipids [57], calcium mobilization [55,58], and induce tropoelastin [59] in ATIIs. Furthermore, applying cyclic mechanical strain (21%, surface area) on primary human pulmonary ATs increases epithelial barrier permeability for small hydrophilic molecules and enhances metabolic activity [60]. The role of amplitude, frequency or uniformity of stretch on these aspects has not been systematically investigated, yet.

Excessive mechanical stretch can also induce apoptosis, phosphatidylcholine secretion, necrosis in ATIIs [61,62] and more severe release of cytokines, especially inflammatory mediators such as Interleukin-8 (IL-8). Vlahakis et al. have reported that excessive cyclic cell stretch (30%, surface area) for up to 48 h upregulated the production and release of IL-8 by human alveolar epithelium (A549 cells) [63].

Moreover, it has been shown that mechanical strain can affect wound healing and wound closure of both airway and alveolar epithelium. Closure was inhibited by excessive mechanical strain such as distention, elongation, and compression [39–41]. In addition to cyclic strain, the combined effects of fluid and interface flows (surface tension) and high transmural pressures during mechanical ventilation can play a role in the development of ventilator-induced lung injury (VILI) especially

in patients who are suffering from ARDS. These aspects can exacerbate lung injury through overdistension of alveolar sacs (volutrauma), cyclic alveolar collapse and expansion (atelectrauma), as well as activation of the inflammatory cascades [64].

In summary, it is evident that cyclic mechanical forces are governing factors in numerous critical regulatory functions of the lung particularly during lung development [65,66].

3. Stretch devices for *in vitro* cell models of the lung

The currently available stretch devices for *in vitro* cell models of the lung can be stratified by their applicability in cell culture conditions i.e. submerged or ALI and by their degree of miniaturization (macro-/microfluidic; **Table 3**). The fundamental concepts of the traditional submerged and the more physiologic ALI cell culture conditions are schematically depicted in Figure 2a and 2b. While in submerged conditions cells are typically attached to plastic wells and culture medium covering the cells, under ALI conditions, epithelial cells are grown on a perforated membrane (typically polyethylene terephthalate, PET) with air on the apical side and cell culture medium on the basal side. ALI cell cultures are a more physiologic model of the lung epithelium as they

- mimic the interfacial function of the epithelial barrier of the lung separating air from interstitial or blood fluid.
- allow for polarization of the epithelial cells which results in a more tightly regulated cell barrier and apical secretion of natural protective liquid layers such as mucus or alveolar lining fluid [67].
- allow for more complex and hence more physiologic multi-cell co-cultures consisting of e.g. epithelial cells with macrophages on the apical side and dendritic or endothelial cells on the basal side of the porous membrane serving as cell support [68–70].

- allow for delivery of airborne gases or aerosols (drugs or toxins) directly to the epithelial cells, which is both conducive for direct measurement of the cell delivered dose via e.g. quartz crystal microbalances [69] and more predictive for clinical outcome than pipetting of these substances into the cell culture medium as done under submerged culture conditions [7,67].

In the following section, we present an overview of the currently available stretch devices for *in vitro* models of the lung epithelium under submerged and ALI cell culture conditions and the more recently introduced microfluidic devices typically referred to as lung-on-a-chip models.

3.1. Devices for submerged cell/tissue culture models

The vast majority of cell-stretching devices described in the literature refer to submerged cell culture models of the lung (Table 3). One of the earliest cellular stretch devices was introduced by Skinner et al. [71–74]. They cultured fetal rat lung cells on a Gelfoam sponge with one side of it fixed to the culture dish and the other end elongated using an electromagnetic field generated by a solenoid unit (Figure 2c). However, the extent of cellular deformation applied by this system was non-uniform and difficult to quantify [11,75].

Another early type of stretch device was used by Wirtz and Dobbs [51,55]. Their device consisted of a flexible poly(dimethylsiloxane) (PDMS, Sylgard 184) membrane on which primary ATIIs were cultured on the apical side and mechanical stretch was applied by changing the hydrostatic pressure below the membrane. However, this device also applied a non-uniform strain to the cells which caused changes in cell behavior due to heterogeneous deformation. In addition, the amount of mechanical stress in this system was adjusted by altering the hydrostatic pressure manually and as a result, this model was not suitable for applying stable cyclic mechanical stretch for an extended period of time.

One of the earliest studies on equibiaxial deformation-induced injury was carried out by Tschumperlin and Margulies who designed a cell-stretching device that applied a uniform, equibiaxial strain to AT cells cultured on a fibronectin-coated non-porous Silastic membranes [75]. An annular indentor was designed to contact the bottom of the silicone membrane (near the rim) and the membrane stretched by moving the indentor. Deformation rate and cycles are regulated by the motor speed (Figure 2d). The strain field (2D, equibiaxial, maximum applied strain 50% surface area) is unchanged during 1 h of continuous cycling (Table 3). This method allowed application of a predictable uniform strain to ATs resulting in more quantifiable investigations of the response of the alveolar epithelium to cyclic mechanical stretch.

This device and other commercially available instruments such as the Flexcell Strain Unit™ (Flexcell International Corporation) and Stretching Apparatus (STREX Inc.) (Table 3) have been utilized by numerous researchers to study the effect of mechanical stretch on ATII [14,61,63,76–78], human pulmonary microvascular endothelial [79] and airway smooth muscle (ASM) [80] cells (Table 2). The general mechanism of the majority of the commercially available cell-stretching devices is based on controlling vacuum pressure underneath the culture plates to apply uniaxial or uniform radial strain to the cell monolayer which is cultured on a flexible silicone membrane (Figure 2e). However, the membranes used in these systems are non-porous due to the application of vacuum on the basal side for stretching the membrane and thus cells cannot be cultured under ALI conditions. Therefore, the *in vitro* devices in these studies do not allow the study of the lung epithelium at ALI which limits their ability to recapitulate the *in vivo* scenario.

In addition to *in vitro* cell culture models, *ex vivo* lung slices have been used to investigate the effects of contraction on ASMs [81]. *Ex vivo* precision-cut lung slices (PCLS) can be derived from human or animal lungs. Lung tissue explants can be processed into lung slices of defined thickness

(200–500 μm; a few alveolar sacs) which are viable up to 5 days [82]. In contrast to in vitro models, PCLS preserve cellular and structural organization of the lung tissue and maintain complex physiologic features not only for healthy, but also diseased lungs [82]. The lung slices can also be stretched to investigate the pulmonary responses to mechanical stretch [83,84]. For instance, the lung slices (PCLS/PDMS: a PDMS membrane used as a supportive layer) were stretched by applying pressure to the basal chamber (biaxial, 0.2 Hz, 4h) [83]. The average stretch was 24.9±4.1% in alveolar perimeter (1D) at 3.5 kPa and 35±8.5% at 5.2 kPa (Table 3).

3.2. Devices for air-liquid interface cell culture models

In recent years, recognition of the previously described advantages of ALI as compared to submerged cell have led to an increase in ALI cell cultures studies with static Transwell® Inserts [69], where epithelial cells are cultured on a *static* porous membrane (typically PET) with air on the apical side and cell culture medium on the basal side (Figure 2b) [85,86]. Only very recently, devices for stretching of ALI cell culture systems have become available (Table 3). Pulmonary cells are normally cultured on rigid substrates (mainly plastic dishes with a stiffness ranging from 2 to 4 GPa) which does not recapitulate the much less stiff basement membranes *in vivo* [87]. For cell stretch under ALI conditions, cells should be grown on membranes which are not only elastic, but also porous for nutrient exchange between apical cells and basal cell culture medium.

To provide better culture conditions during cell seeding and increase the efficiency of cell culturing, bioreactor systems are essential. These systems, allow for tight control of temperature, pressure, and biomechanical stimuli as well as mass transfer of nutrients and oxygen by providing *in vitro* biomechanical and biochemical conditions mimicking *in vivo* conditions [88,89]. Some of these systems are now even capable of studying the responses of ALI cell cultures to mechanical and biochemical cues [90].

Recently, the Moving Air-Liquid Interface (MALI) bioreactor system has been developed to study the role of mechanical stretching on the permeability of epithelial cells to soluble and airborne nanoparticles *in vitro* (Figure 2f). An elastic electrospun membrane made of polycarbonate polyurethane (Bionate®80), where ATIIs are grown under ALI culture conditions, is stretched using air regulation in the apical chamber to mimic natural breathing [91]. However, cell culture was challenging with the Bionate® membrane, even if a highly proliferative lung epithelial cell line (A549) was used.

In the last decade, microfluidic cell-culture platforms (Figure 2g) have been introduced which mimic the main *in vivo* physiological functions and mechanical microenvironment of the alveolar epithelial barrier (Table 3). Microfluidic systems are able to create and regulate small amounts of fluid flows (10^{-9} to 10^{-18} L), and transfer nutrients and other biochemical cues to cells in a controlled manner [92]. In 2009, a continuously-perfused microfluidic system designed to culture human ATs at ALI under dynamic conditions was developed [93]. It has been reported that cells cultured using this platform showed a better degree of monolayer integrity, had higher rates of surfactant production, and lower surface tension of the lining fluid in comparison to the traditional Transwell® culture model. In 2010, Huh and colleagues designed a miniaturized co-culture cell model with microfluidic perfusion [94]. This microsystem is modeled to study functions of the lung by integrating a co-culture of epithelial and endothelial cells on a stretchable, porous PDMS membrane separating the air-filled apical from the liquid-/medium-filled basal compartment of the PDMS bioreactor. Physiologic breathing movements and blood flow have been mimicked by applying cyclic mechanical strain and constant intermittent medium flow on the apical and basal side of the *in vitro* alveolar barrier, respectively [94]. Although this multifunctional microdevice may provide superior culturing conditions for human lung cells rather as compared to conventional

culture systems, it does not fulfill all of the characteristics of the alveolar-capillary barrier *in vivo*, such as barrier thickness (PDMS membrane is 10 μm; alveolar tissue barrier < 1 μm thick). Moreover, it does not include all of the major cell types native to the lung and can therefore hardly be considered as a lung-on-a-chip, but a miniaturized version of the widely used 2D co-culture models of the lung. Recently, a new version of this device updated to regenerate a 3D cross-section of a human lung alveolus (co-culturing of primary human ATs (mixture of type I and II) with human umbilical vascular endothelial cells (HUVECs)); but, not subjected to cyclic mechanical stretch [95].

Another simplified microfluidic device was designed to mimic obstructive sleep apnea (OSA) for studying cellular responses to cyclical hypoxia and stretch [96]. They showed that hypoxia-inducible factor 1α is upregulated in mesenchymal stem cells under both intermittent hypoxia and cyclic stretch. The circular PDMS membrane of this device is stretched over a rigid post resulting in two regions with uniform but different strain profile. While in the center region (on post), there is uniform radial strain with an added circumferential strain field, the circumferential strain is small in the off-post region (rim) [97]. In fact, this is a common limitation with other commercial stretchable devices such as Bioflex® culture plates (Flexcell International Corporation, Burlington, NC) [97]. Hence, for cell experiments under identical uniform strain conditions only the on-post region of the membrane should be populated with cells.

In 2015, another microplatform was designed which sought to recreate the pulmonary parenchymal environment to investigate the effects of breathing movements on human primary cells derived from patients [60]. In this perhaps most physiological lung-on-a-chip microdevice to date, the membrane is actuated indirectly (3D, tri-axial) using a bio-inspired microdiaphragm located at the bottom of the basolateral chamber (Figure 2h). Cells are seeded on a surface modified (oxygen

plasma) and fibronectin-coated porous PDMS membrane (thickness is 10 μm; pore size 3 or 8μm). After that, a cyclic mechanical stretch is applied to the PDMS membrane (21%, 2D, at frequency of 0.2 Hz) by exerting a negative pressure. The modified version of this model enables online monitoring of transepithelial electrical resistance (TEER) in real-time using a microimpedance tomography system (at a distance of 1mm from the electrodes) [98]. In addition, the microfluidic device used in this study can be equipped with a passive medium exchange unit to provide long-term culture conditions under ALI [99,100].

In summary, there has been substantial progress towards establishing an *in vitro* cell culture model of the lung which mimics an increasing number of the core features of the lung including mechanical stretch and ALI conditions. A silicone-based membrane is commonly used in commercially available devices and microfluidic studies. Even after coating with ECM proteins (such as collagen, fibronectin, and mixtures of ECM proteins such as Matrigel), epithelial cells do not always grow to a complete confluent cell layer on these hydrophobic membranes and if they do then one often finds multi-layered regions, which are a poor model of the monolayered lung epithelium. In addition, other biophysical parameters of the membrane such as porosity and thickness are very essential for cell proliferation and *in vivo*–like permeability of the *in vitro* air-blood (alveolar-capillary) barrier. Therefore, there is a need to design more biomimetic membranes which more closely mimic the physiological aspects of the native basement membrane.

4. Alveolar-capillary basement membrane for ALI cell cultures

For submerged cell culture conditions, stretchable cell support membranes are mainly selected based on elasticity, wettability, durability, biocompatibility, and availability (cost). However, alveolar epithelium represents the ALI with air on the apical side and tissue/liquid on the other basal side. ALI conditions can be mimicked under *in vitro* conditions by seeding cells on a

permeable membrane allowing for contact with air from the apical side and nutrient supply with cell culture medium from the basal side via the permeable membrane. Therefore, to manufacture an appropriate membrane for ALI conditions, additional biophysical parameters such as porosity, permeability, and multi-cellular compatibility should be considered. In addition, compatibility with optical imaging techniques (e.g. confocal microscopy) is a desirable, albeit not absolutely necessary feature of the membrane.

Various membrane materials and manufacturing techniques have been assessed for lung tissue as summarized in **Table 4**. Currently, silicone-based materials such as PDMS are by far the most favored material type due to its high compliance with a Young's modulus of ca. 1–3 MPa (however, also values below 1 MPa are possible depending on base to cross-linker ratio [101]), as well as good gas permeability, optical transparency, low cost, and ease of use [102,103]. However, silicone is known to be highly adsorptive towards many small and large molecules relevant for drug testing or nourishment of the cells, which renders it problematic for drug transport studies and cytokine release monitoring in the basal compartment [103,104]. Alternative approaches such as electrospun membranes made of various materials (e.g. polycarbonate polyurethane (PCU) [91], polycaprolactone (PCL) [105], polydioxanone (PDS) [106], and poly(lactic-co-glycolic acid) (PLGA) [107]) yielded acceptable results in terms of stretch conditions, but often suffer from limitations regarding cell growth and proliferation due to the hydrophobic nature of these materials, which cannot be completely eliminated even after coating with ECM proteins (such as collagen and fibronectin [108]). As a consequence, the selection of a suitable membrane has been one of the most challenging aspects in the development of stretch-actuated, ALI lung bioreactors.

4.1. Membrane properties

Ideally, the biophysical properties of membranes used for stretch-activated bioreactors of the lung should closely mimic the native basement membrane of the alveolar-capillary barrier, which have been summarized in Table 1. Careful consideration and close matching of these physiologic parameters is essential for membrane design yielding biomimetic culture conditions for pulmonary cells. Collating physiologic properties with technical limitations of current membrane technologies results in a list of membrane characteristics guiding the selection of membrane material and fabrication as summarized in Figure 3d.

As mentioned above elasticity or stiffness is among the most important membrane characteristic. However, compliance of the membrane should also be considered, i.e. the membrane should be elastic enough to endure prolonged cyclic mechanical stretch (for at least days) with an amplitude of up to 12% (1D) or even 20% (pathological conditions) without experiencing plastic deformation, creep or rupture [109] under realistic cell culture conditions (contact with cell culture medium). Moreover, a sufficiently high degree of wettability with contact angles below 70° is desirable for the growth of confluent epithelial and endothelial cell monolayers as encountered at the air-blood interface. Wettability (hydrophilicity/hydrophobicity) is governed by surface characteristics of the membrane including charge, chemistry, and roughness of the membrane [110–112]. Membrane permeability governed by porosity and pore interconnectivity is also in important aspect of membrane design as it is essential for various processes facilitating cell growth such as nutrient absorption, and metabolic waste removal [113,114], but also for cell-cell signaling processes. Cells secrete signaling molecules (e.g. interleukins) and extracellular vesicles (e.g. exosomes) across the basement membrane under both homeostatic and pathological conditions, but also in response to environmental challenges including pathogens, gaseous irritants, cigarette smoke, and environmental particles [115,116]. Monitoring of these cell signaling processes is vital for

understanding the role of cell signaling in disease development and requires the use of porous membrane.

Transport rates are a function of membrane porosity and thickness [117]. As stated above the air-blood barrier can be considered as a permeable membrane with submicron thickness (0.62 μm) perforated with nano-sized pores (<2.5 nm in diameter [33] (Table 1, Figure 3c). For *in vitro* cell cultures, size and topography of the pores in the membrane need to be large enough to achieve desirable gas and nutrient exchange between apical and basal compartment (at least 10 nm diameter for large biomolecules to pass through), but small enough to prevent inadvertent cell migration across the membrane (<3 – 8 μm depending on cell type). Hence, the most widely used pore size of ca. 3 μm facilitates the formation of epithelial-endothelial cell bilayers mimicking the alveolar-capillary barrier, while allowing transport of nutrients, growth factors and cell signaling molecules (e.g. cytokines, chemokines, and extracellular vehicles) at physiologic rates [118–121]. Another major factor in mimicking the properties of the air-blood barrier of the lung is its thickness ca. 0.6 μm in the gas exchange region [35]. On the other hand, the human basement membrane in the alveolar-capillary region is only ca. 0.6 μm thick (Table 1). Since submicron membranes, are difficult to handle, the majority of artificial membranes reported in the literature are in the 10-micron range. The increased membrane thickness results in additional resistance to respiratory gas and macromolecular exchange and hence remains a major limiting factor in the design of biomimetic membranes for *in vitro* approaches to the alveolar-capillary barrier.

4.2. Membrane fabrication

Membrane fabrication is one of the key determinants of membrane properties. The conventional techniques for porous membrane fabrication are phase separation [122], self-assembly [123], freeze-drying [124], solvent casting [125], and electrospinning [126].

Thermally induced phase separation is a convenient technique for casting a wide range of polymers such as PLLA and PLGA into an interconnected porous film [127]. This method is easy to use, reproducible and obtained membranes have high porosity and narrow pore size distribution. However, control of pore size and shape is difficult due to the lack of control over fiber arrangement [127,128].

Solvent casting is a simple and inexpensive way to manufacture a porous scaffold, albeit further modifications are required to overcome innate abnormal pore shape and interconnectivity [129]. Organizing and arranging materials by molecule or self-assembly is another way to fabricate a porous membrane. With this method, the physical and structural properties of nanofibers can be controlled by oligopeptide composition and chemistry. However, limited choice of proper molecules and lack of control over pore size and shape are the main disadvantages of this 'bottom-up' approach [130,131].

Electrospinning stands out as a powerful method in creating porous membranes that resemble the fibrous architecture of natural ECM [132]. Electrospinning is a versatile technique, which can be applied to virtually any polymer as well as many macromolecules, reshaping a rich library of materials into fibers with a diameter ranging from a few nanometers to micrometers. The nano/micro scale fibrous morphology of the scaffolds provides a unique high surface area to volume ratio [133], which is one of the main parameters that affects the surface area and overall porosity of the membranes, together with packing density. Intricate interplay between process and solvent parameters such as feeding rate, voltage, concentration and choice of solvents, enables control over the fiber size [132]. In addition, membrane porosity can be further increased via salt leaching [134] and sacrificial polymers, [135] whereas the packing density of fibrous membranes can be tailored via electrostatic repulsion [136] and wet electrospinning [137]. It should be noted that the

choice of the material, e.g. hydrophobic/hydrophilic, is to be considered in the context of fiber morphology and permeability analysis, which will be addressed in more detail below [138]. Manipulation of the shape of the electrospun fibers can be utilized to match the mechanical features, required by the lung-tissue models, such as stiffness and elasticity. Previously, lower packing density in electrospun fibers was reported to decrease the bulk stiffness of the membranes [139]. Moreover, fabrication of coiled fibers allowed increased stretchability/extensibility compared to straight fibers and further contributed to the contraction of cardiomyocytes [140]. Such mechanical actuation capacity may prove useful for the cyclic stress mimicry in *in vitro* lung tissue models.

Furthermore, bioprinting technology engaging cells, growth factors, and biomaterials (synthetic and natural ECM) is another promising strategy to maximally mimic the alveolar-capillary tissue. In the study that is first of its kind, Horvath et al. engineered an air-blood barrier via layer by layer bioprinting of endothelial and epithelial cells that are separated with a thin layer of Matrigel which mimics the basement membrane in the native lung tissue [141]. Both types of printed cells exhibited high viability and formed into thin confluent monolayers which facilitated necessary cell-cell interactions. The authors suggested that the reproducible biofabrication of such air-blood barrier could serve as a high-throughput screening platform for safety assessment and drug efficacy testing. Recently, an even more applied study reported bioprinting of A549 cells into 3D cell-laden constructs [142]. Once the printability, structural stability and cell friendliness of the bioinks were established, the infection patterns were analyzed for a seasonal influenza A strain [142]. The authors concluded that the virus was distributed throughout the 3D printed structure and caused a clustered infection pattern that is comparable to the natural infection in the lung tissue, which cannot be replicated with traditional 2D cell culture models.

Bioprinting is a rapid production technique which provides powerful control over the fabrication process and patterning. However, it is in an early technological phase of development and high-resolution cell patterning and distribution are among its main technical challenges. In addition, selecting a tunable biocompatible material is another concern for bioprinting to achieve an appropriate resolution in a scale of the air-blood barrier [143,144].

4.3. Material selection

The type of material is another controlling factor of membrane features. Polymers are as the most widely used type of biomaterials because of their diversity in chemical groups which allows fine-tuning of unique physical properties such as high surface-to-volume ratio, high porosity, and mechanical property [145,146]. A wide variety of synthetic and natural-based materials and composite materials (natural-synthetic hybrids) has been employed to obtain a thin scaffold which is appropriate for soft tissue applications (Table 4).

One of the most widely used synthetic-based materials is PCL which is a biodegradable, biocompatible, and bioresorbable polymer. PCL scaffold can be manufactured by various fabrication methods due to its breadths in rheological and viscoelastic properties [105]. In addition to PCL, other synthetic-based polymers such as polyethylene terephthalate (PET) [147,148], PCU [91] have been used to culture epithelial cells. Besides, PDS has been broadly used [149–151] in tissue engineering applications as a biodegradable polymer with a relatively fast degradation rate. PDS shows enhancing cell infiltration and tissue regeneration when grafted with low-degradation rate polymers such as PCL in which large pore spaces created by degradation of PDS [106]. Synthetic-based polymers have many advantages including suitable mechanical properties, tunable biodegradability, easy sourcing, great flexibility in synthesis and modification, and - last but not least - low cost.

However, synthetic polymers lack cell affinity because of their low hydrophilicity and lack of surface cell recognition sites [152,153]. To overcome this drawback, synthetic-based materials are often functionalized prior to biological use. Hydrophilicity can be enhanced via several ways including plasma and polyvinyl alcohol (PVA) treatment, chemical coupling of hydrophilic polymers either via copolymerization or surface grafting, surface patterning, and preparing hydrophobic/hydrophilic polymer blends [108,154]. Membranes with appropriate hydrophilicity promote adsorption of ECM proteins, secreted from the seeded cells, without interfering with their functional/physiological conformation and thus render the scaffold bioactive [155,156]. Direct inclusion of (natural) bioactive molecules offers the possibilities to overcome the lack of surface cell recognition sites in synthetic-based polymers. The most common bioactive molecules are ECM proteins, such as collagen (or gelatin as surrogate), laminin, fibronectin, and elastin or other protein-based materials such as silk [108]. Such natural polymers can provide better cell-matrix interactions and biocompatibility as compared to synthetic-based polymers. However, natural polymers tend to display poor processing ability, batch to batch variance and poor mechanical properties such as elasticity, stiffness and durability [157]. Although mechanical features of natural-based polymers can be improved with an additional crosslinking process [158], using membranes solely composed of natural-based polymers is likely not suitable for long-term culturing of cells under mechanically challenging conditions like cyclic stress.

Instead, natural/synthetic composite materials can be formulated to exploit bioactive features of biologic materials combined with tunable/stable mechanical features of synthetic-based polymers. In a recent study, an electrospun PCL/gelatin polymer blend was fabricated to mimic ECM and study the effect of ECM mechanics and topography on alveolar-capillary barrier permeability and cell injury during airway reopening [159]. In this study, a non-biological polymer (PCL) not only

provided elasticity and mechanical durability but also allowed for better control of membrane production (various PCL/gelatin mixtures yielded elastic modulus: 0.36-7.20 MPa) (Table 4). The manufactured membranes were used to study surface tension forces during airway reopening. Other natural-synthetic hybrid polymers such as PDS/gelatin/elastin [151], PLGA/gelatin/elastin [107], and collagen/P(LLA-CL) [160] have shown good biocompatibility, mechanical properties and other physical characteristics desirable for *in vitro* models of the alveolar-capillary membrane.

Alternatively, cell adhesion peptides derived from ECM proteins, such as RGD (arginylglycylaspartic acid) and IKVAV (isoleucine-lysine-valine-alanine-valine), can be immobilized on synthetic polymers to create selectively bioactivated synthetic membranes. Employing short peptide sequences rather than whole proteins offers tailor-made synthesis options and efficient/precise conjugation possibilities, which increase the overall impact of the functional epitopes [161,162]. Although bioactive peptides can be directly blended with the polymers, chemical conjugation assures more reproducible and stable bioactivation. Among various conjugation methods, carbodiimide chemistry, Michael-addition, and photo-initiation based reactions are widely reported [163–165]. It has also been demonstrated that covalent chemical coupling of peptides can be achieved *in-situ* through the application of a reactive hydrophilic additive to hydrophobic polyesters in the spinning solution [166]. Grafahrend et al. [166] conjugated the cell adhesion peptide GRGDS to a reactive hydrophilic pre-polymer, NCO-sP(EO-stat-PO) already in the solution that was used for electrospinning. Subsequent co-spinning of bioconjugated NCO-sP(EO-stat-PO) with PLGA rendered electrospun fibers hydrophilic, reduced the unspecific protein adsorption and cultivated strong cell-substrate adhesion. In a similar way, Rossi et al. fabricated electrospun membranes which mimicked the bipolar structure of the basement membrane by conjugating ECM proteins (collagen IV, fibronectin and laminin) to NCO-sP(EO-stat-PO). A bipolar membrane is

then fabricated through subsequent spin-coating with solutions, bioconjugated with different ECM derived peptide sequences [167].

Bioactivated fibrous membranes supported the bipolar co-culture of keratinocytes and fibroblast, mimicking the basal and reticular side of the basement membrane. A similar approach can be utilized for capturing the bipolar structure of the pulmonary epithelial barrier. Most recently, this approach has been extended to combine ECM-peptide bioconjugation with the covalent immobilization of biochemically active molecules such as antibodies to combine selective cell adhesion with, in this case, immunomodulatory effects [168].

Furthermore, it has been shown that decellularized extracellular matrix (dECM) containing essential proteins for cell attachment and proliferation, could be a good candidate to improve the biocompatibility of copolymers [169,170]. In a recent study, hybrid electrospun scaffold of poly-l-lactic acid (PLLA) and dECM (derived from pig lung) for *in vitro* ASM model showed that dECM improved physical characteristics (e.g. wettability) [171].

PDMS is the most widely used membrane material for *in vitro* cell-stretching devices of the alveolar-capillary barrier (section 3). However, inadvertent adsorption of small molecules onto the surface of PDMS can affect cellular responses or prohibit drug transport studies. Copolymers (natural and synthetic-based) have been suggested to overcome the limitations of PDMS-based membranes. However, relatively few studies are available demonstrating successful cell culturing on these membranes both at the ALI and under cyclic mechanical stretch as encountered at the alveolar-capillary barrier.

In summary, it is evident that there is a need for development of alternative materials suitable for manufacturing a biocompatible, porous, thin, and stretchable membrane mimicking the physiologic parameters of the native basement membrane of the alveolar-capillary barrier.

Moreover, the optimum choice of manufacturing method will also play a crucial role for obtaining the most biomimetic properties. The optimum material and processing techniques should ideally result in a final product that is not only bioactive enough to facilitate a fully confluent cell monolayer on the membrane but also meet the high requirements on mechanically properties and chemical integrity for long-term studies with lung tissue models.

5. Future directions: biomimetic models of the lung

Currently, the vast majority of *in vitro* efficacy, toxicity and pharmacokinetics studies of the lung are performed using static pulmonary cell models culturing a single cell type under submerged conditions [172,173]. While this approach is well established, it often lacks predictive power for *in vivo*/clinical outcome due to non-physiologic and simplistic cell model conditions and an unknown dose of the test substance delivered to the cells [7,67]. Recent advances in biomimetic lung models include ALI culture conditions (polarization of epithelial cells at the ALI), apical coverage of epithelial cells with lung lining fluid (surfactant and alveolar lining fluid), and multiple-cell co-culture models providing more biomimetic barrier function (epithelial and endothelial cells), immune competence (dendritic cells), and clearance capability (macrophage, mucus) [14,67]. With the availability of commercial aerosol-cell delivery systems (e.g. VITROCELL CLOUD, Precise Inhale, and CULTEX technology), an increasing number of studies employs aerosolized drug/substance delivery for more realistic pharmacokinetics and dose-response measurements [174]. Any of these aspects enhances the biomimetic characteristics of *in vitro* cell models but depending on the endpoint of interest either all or only a subset of them may have to be included for adequate prediction of *in vivo* outcome. Unraveling the link between *in vitro* prediction of certain *in vivo* endpoints and the most suitable lung models will remain a field of intense research.

Moreover, there is also a trend towards microfluidic platforms of *in vitro* lung models offering the perspective of optimized process control, more efficient substance use, real-time monitoring systems via computer-control and automation ultimately leading to high-throughput capabilities [18]. Analogous to standard cell culture systems and bioreactors, these micro-platforms are also able to mimic certain aspects of the pulmonary parenchymal environment such as epithelial-endothelial barrier, ALI, and mechanical stimulation induced by breathing and blood perfusion. However, these so-called lung-on-a-chip devices are often not easy to handle, provide a relatively small number of cells limiting the available amount of sample for biological (multi-omics) analysis. This may at least partially explain why there are very few lab-on-a-chip devices commercially available, yet.

Notwithstanding even more advanced technologies are already pursued such as more complex 3D organ-specific cell structures representing functional organ units (organoids) and the integration of organ-specific chips/organoids into *in vitro* organism systems. Although these methods are still in an early stage, they hold the promise to overcome remaining shortcomings of current advanced *in vitro* models of the lung such as failure of fully mimicking the complexity of the 3D alveolar structure, the multi-cell interplay in the lung (ca. 60 different cell types) and inter-organ connectedness via blood circulation [175,176].

In addition to these so-called bottom-up approaches, where biomimetic organ-specific models are built up from single-cell structures, also top-down approaches are available, where the lung (or a single lobe) is cut into smaller tissue slices [7]. These *ex vivo* PCLS models, which can also be used under dynamic stretch conditions, represent a thin slice of the multi-cell 3D architecture of the lung which has been shown to maintain physiologic functions such as ciliary beating, macrophage migration and response to e.g. pro-inflammatory stimuli [177,178]. Among other applications, PCLS

have been used to study pathological and therapeutic measures of COPD/emphysema in lung tissue [82], and more recently to visualize the location and migration of different cell types in the lung tissue such as dendritic cells [179]. Lung slices with a supportive layer such as PDMS have been exerted to cyclic mechanical stretch without causing cell injury [83]. However, even this complex 3D multi-cell model of the lung can only partly reflect the properties of native lung tissue. For instance, it does not represent an intact epithelial-endothelial tissue barrier, ALI conditions as encountered in the lung and an intact immune system causing non-physiological responses [180]. Moreover, these top-down approaches still require the use of animals or donor organs, while bottom-up approaches bear the potential of animal free drug/toxicity testing.

All of these developments towards more biomimetic, miniaturized and complex models of the lung will benefit from the implementation of cyclic mechanical stretch as one of the fundamental stimuli in the lung. Until now, commercially available cell-stretching devices have only been available for submerged, but not for more physiologic ALI cell culture conditions. The suggested technologies for cell-stretching under ALI conditions mainly rely on silicone-based membranes such as PDMS [181,182], which have plenty of advantages such as good compliance and permeability. However, due to the hydrophobic nature of PDMS, surface modifications or ECM protein coatings are required to enhance cell adhesion and biocompatibility [183,184]. However, the hydrophobic nature of PDMS requires surface modifications s such as coating with ECM proteins for adequate cell grow. But even then, multilayered or nonconfluent monolayered cell regions can often not be avoided [11]. In spite of these efforts, PDMS membranes may adversely affect cellular response even for short-terms studies (1h) [102] and silicone-based materials are known for their adsorptive nature and hence their potential bias when considering transmembrane transport of drugs and biomolecules [103,104]. The latter is not the case for PET membranes implemented in the standard

Transwell® insert technology used for static ALI cell cultures. However, PET is not elastic and hence not suitable for mimicking cyclic stretch. Hence, neither PET nor silicone-based materials meet all of the requirements of a biomimetic basement membrane. In principle, the next generation of ALI cell culture membranes for even more physiologic *in vitro* models of the lung should also mimic the curvature of the alveolar epithelium (alveolar diameter: ca. 250 μm) and the interaction between cells and ECM.

As discussed above the essential characteristics of suitable basement membranes include porous architecture, dimension, biocompatibility, stiffness, and permeability. The physiologic parameter range of these parameters is summarized in Table 1. A thin (ideally <1 μm) and porous membrane is required to mimic the structural and mechanical properties of the alveolar wall supporting growth and maintenance of an intact epithelial monolayer under ALI culture conditions. Thus, designed membranes should have sufficient elasticity, durability for long-term stretch in cell culture systems and act as cell substrate as well as allow for nutrient exchange between basal and apical compartment.

At this time, there is no widely accepted material meeting all of the physiologic requirements for the native basement membrane of the alveolar-capillary barrier (Table 1). However, there is evidence that rather than using a single material the application of hybrid copolymers may prove advantageous for representing all of the desired mechanical and biophysical properties. Among them, scaffolds obtained by PCL [185,186] and P(LLA-CL) [109] blended with natural-based polymers such as gelatin [159,187], collagen [160], and elastin [188] showed a suitable porosity and surface hydrophilicity. Blends of PCL/natural polymers met the mechanical properties such as elasticity, reversible elongation and energy absorbed up to the elastic point reported for the basement membrane in the alveolar region. Other synthetic polymers such as P(LLA-CL) also showed

appropriate mechanical properties for soft tissue applications [160,189,190]. For instance, electrospun hybrid scaffolds of collagen/ P(LLA-CL) has been used for application of cardiovascular tissue engineering [160]. The hydrophilicity, biocompatibility, and mechanical properties (Young's modulus: 1.77±0.09 MPa) of these hybrid materials make them promising membrane materials for lung models, although they have not been widely applied in lung research, yet. dECM-derived native lung tissue, a biomimetic mixture of natural ECM proteins, is another promising natural material because of its excellent biocompatibility features, although it does not have sufficiently biomimetic mechanical properties [170]. As this deficiency can be compensated by hybridization with a synthetic polymer, several synthetic/dECM copolymers have been recently manufactured for tissue engineering application [191–193].

In addition to selecting a proper (composite) material which fulfills the physiologic properties of the alveolar basement membrane, fabrication methods should also be considered. Electrospinning is a simple and cost-effective technique which enables control over the shape, thickness, architecture and biophysical characteristics of the scaffold. A tunable porous structure with a high surface area to volume ratio, mimicking natural ECM in native tissues, can be manufactured within this method. However, poor cellular infiltration is still the main limitation of electrospun scaffolds which can be improved somewhat when combined with other techniques such as phase separation and solvent casting [194,195].

Moreover, biofabrication is a young and vibrant field of research which offers great potential for the generation of skin and lung tissue. This technique aims at the generation of biological functional tissue analogs either through an automated assembly of cell-containing building blocks, or by bioprinting of cells, biomaterials, and biologically active factors into 3D constructs [209]. Bioprinting inherently requires a bioink, a cell-containing formulation that can be processed by a

suitable technology [196,197]. The design and application of bioinks have expanded greatly in the last decade, with numerous materials – primarily natural and synthetic hydrogels – being applied or developed to meet the stringent demands of bioprinting [198,199].

Recently, an endothelium-epithelium along with basement membrane has been fabricated using a layer-by-layer method in order to mimic the pulmonary air-blood tissue barrier [141]. A 3D bioprinted tissue model employing cell-laden bioinks has been also used as a model for studying influenza infection in the lung [142]. These examples clearly show the potential of biofabrication for the engineering of functional lung tissue. However, many challenges still need to be overcome, such as the development of materials and techniques that specifically suit lung cells forming the bipolar architecture of an air-blood barrier and providing mechanically tuned constructs that mimic the dynamic nature in native lung tissue.

6. Conclusions

Mechanical forces play a key role in proliferation, differentiation, function, and metabolism of lung cells. The main stretch-related regulatory pathways include the MAPK/ERK- and cAMP-PKA-dependent signaling pathways triggering differentiation of ATIIs as well as activation of YAP/TAZ and the signaling cascade of Cdc42/F-actin/MAPK controlling alveolar regeneration. The main stretch- and permeability-related physiologic parameters of the native basement membrane of the alveolar-capillary tissue are the level of mechanical linear (1D) strain (4-12%; up to 20% under pathological conditions), elasticity (1-2 kPa), thickness (ca. 50 nm), and porosity (pore size <2.5 nm) and thickness (ca. 0.6 μm; total air-blood barrier). In addition to matching these biophysical conditions, suitable *in vitro* membranes for pulmonary cell-stretching also require biocompatibility, which includes wettability (WCA <70°) and conduciveness to cell growth.

Meeting all of these biophysical parameters in current *in vitro* systems is a challenge, which has not yet been fully accomplished. The currently available body of *in vitro* data on the effects of cyclic mechanical stretch on lung biology was almost exclusively obtained for non-physiologic submerged cell culture conditions using non-porous silicon-based membranes (e.g. PDMS). Even the few currently proposed systems for pulmonary cell-stretching under more physiologic ALI culture conditions mainly rely on super-micron thick silicone membranes (even the microfluidic systems) with micron-sized pores. Moreover, silicone has well known material-specific deficiencies such as limited biocompatibility (requires surface treatment) and capturing of relevant biomolecules and potentially applied drug molecules, which poses serious limitations for drug efficacy and pharmacokinetics studies.

Our review of natural and synthetic-based polymers revealed that natural/artificial hybrid materials combine high biocompatibility (natural-based polymers) with favorable mechanical properties (artificial polymers) for soft tissue membrane applications such as alveolar tissue models. For the lung, PCL and P(LLA-CL) have been identified as appropriate synthetic-based polymer candidates, while collagen, dECM and gelatin may qualify as suitable natural-based polymer components. Further research into the exact ratio of natural-artificial copolymers is required to obtain the most suitable membrane for next generation, ALI, cell-stretching bioreactors of the lung.

Acknowledgments

The authors are grateful to Prof. Ewald Weibel for the electron microscopy images. Sinem Tas is supported by a RESPIRE3 Postdoctoral Fellowship supported by the European Respiratory Society and the European Union's H2020 research and innovation programme under the Marie Sklodowska-Curie grant agreement (No 713406). The Knut and Alice Wallenberg foundation is acknowledged for generous support (DEW). This project has received funding from a European

Research Council (ERC) Starting Grant under the European Union's Horizon 2020 research and innovation programme (grant agreement No 805361)(DEW).

References

[1] U. Hatipoğlu, *Ann. Thorac. Med.* **2018**, *13*, 1.
[2] R. Beasley, A. Semprini, E. A. Mitchell, *Lancet* **2015**, *386*, 1075.
[3] S. M. May, J. T. C. Li, *Allergy Asthma Proc.* **2015**, *36*, 4.
[4] C. A. Pope, M. Ezzati, D. W. Dockery, *N. Engl. J. Med.* **2009**, *360*, 376.
[5] J. G. Muscedere, J. B. Mullen, K. Gan, A. S. Slutsky, *Am. J. Respir. Crit. Care Med.* **1994**, *149*, 1327.
[6] K. Zscheppang, J. Berg, S. Hedtrich, L. Verheyen, D. E. Wagner, N. Suttorp, S. Hippenstiel, A. C. Hocke, *Biotechnol. J.* **2018**, *13*, 1700341.
[7] C. Darquenne, J. S. Fleming, I. Katz, A. R. Martin, J. Schroeter, O. S. Usmani, J. Venegas, O. Schmid, *J. Aerosol Med. Pulm. Drug Deliv.* **2016**, *29*, 107.
[8] D. J. Riley, D. E. Rannels, R. B. Low, L. Jensen, T. P. Jacobs, *Am. Rev. Respir. Dis.* **1990**, *142*, 910.
[9] M. E. Chicurel, C. S. Chen, D. E. Ingber, *Curr. Opin. Cell Biol.* **1998**, *10*, 232.
[10] M. Liu, J. Xu, P. Souza, B. Tanswell, A. K. Tanswell, M. Post, *Vitr. Cell. Dev. Biol. - Anim.* **1995**, *31*, 858.
[11] H. R. Wirtz, L. G. Dobbs, *Respir. Physiol.* **2000**, *119*, 1.
[12] X. Trepat, *AJP Lung Cell. Mol. Physiol.* **2006**, *290*, L1104.
[13] X. Trepat, M. Grabulosa, F. Puig, G. N. Maksym, D. Navajas, R. Farré, *Am. J. Physiol. Cell. Mol. Physiol.* **2004**, *287*, L1025.
[14] R. L. Heise, V. Stober, C. Cheluvaraju, J. W. Hollingsworth, S. Garantziotis, *J. Biol. Chem.* **2011**, *286*, 17435.
[15] N. Gueven, B. Glatthaar, H.-G. Manke, H. Haemmerle, *Eur. Respir. J.* **1996**, *9*, 968.
[16] K. A. Birkness, M. Deslauriers, J. H. Bartlett, E. H. White, C. H. King, F. D. Quinn, *Infect. Immun.* **1999**, *67*, 653.
[17] T. H. Petersen, E. A. Calle, L. Zhao, E. J. Lee, L. Gui, M. B. Raredon, K. Gavrilov, T. Yi, Z. W. Zhuang, C. Breuer, E. Herzog, L. E. Niklason, *Science (80-.).* **2010**, *329*, 538.
[18] A. Doryab, G. Amoabediny, A. Salehi-Najafabadi, *Biotechnol. Adv.* **2016**, *34*, 588.
[19] A. Doryab, M. Heydarian, G. Amoabediny, E. Sadroddiny, S. Mahfouzi, *J. Med. Biol. Eng.* **2017**, *37*, 53.
[20] D. E. Gorman, T. Wu, S. E. Gilpin, H. C. Ott, *Tissue Eng. Part C Methods* **2018**, *24*, 671.
[21] A. Patwa, A. Shah, *Indian J. Anaesth.* **2015**, *59*, 533.
[22] V. D. Varner, C. M. Nelson, *Development* **2014**, *141*, 2750.
[23] B. Suki, S. Ito, D. Stamenović, K. R. Lutchen, E. P. Ingenito, *J. Appl. Physiol.* **2005**, *98*, 1892.
[24] E. Roan, C. M. Waters, *Am. J. Physiol. - Lung Cell. Mol. Physiol.* **2011**, *301*, L625.
[25] J. B. Forrest, *J. Physiol.* **1970**, *210*, 533.
[26] J. J. Fredberg, R. D. Kamm, *Annu. Rev. Physiol.* **2006**, *68*, 507.
[27] *Ann. ICRP* **1994**, *24*, 1.
[28] C. M. Waters, E. Roan, D. Navajas, In *Comprehensive Physiology*; John Wiley & Sons, Inc.: Hoboken, NJ, USA, 2012; Vol. 33, pp. 48–56.
[29] O. T. Guenat, F. Berthiaume, *Biomicrofluidics* **2018**, *12*, 042207.
[30] E. R. Weibel, *Respir. Physiol.* **1970**, *11*, 54.
[31] A. Taylor, Gaar KA, *Am. J. Physiol. Content* **1970**, *218*, 1133.
[32] P. N. Lanken, J. H. Hansen-Flaschen, P. M. Sampson, G. G. Pietra, F. R. Haselton, A. P. Fishman, *J. Appl. Physiol.* **1985**, *59*, 580.
[33] C. Hermans, A. Bernard, *Eur. Respir. J.* **1998**, *11*, 801.
[34] E. R. Weibel, *Swiss Med. Wkly.* **2009**, *139*, 375.
[35] P. Gehr, M. Bachofen, E. R. Weibel, *Respir. Physiol.* **1978**, *32*, 121.
[36] B. C. Goss, K. P. McGee, E. C. Ehman, A. Manduca, R. L. Ehman, *Magn. Reson. Med.* **2006**, *56*, 1060.
[37] A. J. Booth, R. Hadley, A. M. Cornett, A. A. Dreffs, S. A. Matthes, J. L. Tsui, K. Weiss, J. C. Horowitz, V. F. Fiore, T. H. Barker, B. B. Moore, F. J. Martinez, L. E. Niklason, E. S. White, *Am. J. Respir. Crit. Care Med.* **2012**, *186*, 866.
[38] N. F. Jufri, A. Mohamedali, A. Avolio, M. S. Baker, *Vasc. Cell* **2015**, *7*, 8.

[39] C. M. Waters, M. R. Glucksberg, E. P. Lautenschlager, C.-W. Lee, R. M. Van Matre, R. J. Warp, U. Savla, K. E. Healy, B. Moran, D. G. Castner, J. P. Bearinger, *J. Appl. Physiol.* **2001**, *91*, 1600.
[40] L. P. Desai, K. E. Chapman, C. M. Waters, *Am. J. Physiol. Cell. Mol. Physiol.* **2008**, *295*, L958.
[41] U. Savla, C. M. Waters, *Am. J. Physiol.* **1998**, *274*, L883.
[42] P. G. Smith, K. E. Janiga, M. C. Bruce, *Am. J. Respir. Cell Mol. Biol.* **1994**, *10*, 85.
[43] P. R. Chess, L. Toia, J. N. Finkelstein, *Am. J. Physiol. Cell. Mol. Physiol.* **2000**, *279*, L43.
[44] L. S. Chaturvedi, H. M. Marsh, M. D. Basson, *Am. J. Physiol. Physiol.* **2007**, *292*, C1701.
[45] J. Sanchez-Esteban, Y. Wang, P. A. Gruppuso, L. P. Rubin, *Am. J. Respir. Cell Mol. Biol.* **2004**, *30*, 76.
[46] Y. Wang, B. S. Maciejewski, N. Lee, O. Silbert, N. L. McKnight, J. A. Frangos, J. Sanchez-Esteban, *Am. J. Physiol. Cell. Mol. Physiol.* **2006**, *291*, L820.
[47] Z. Liu, H. Wu, K. Jiang, Y. Wang, W. Zhang, Q. Chu, J. Li, H. Huang, T. Cai, H. Ji, C. Yang, N. Tang, *Cell Rep.* **2016**, *16*, 1810.
[48] S. Piccolo, S. Dupont, M. Cordenonsi, *Physiol. Rev.* **2014**, *94*, 1287.
[49] C. C. dos Santos, B. Han, C. F. Andrade, X. Bai, S. Uhlig, R. Hubmayr, M. Tsang, M. Lodyga, S. Keshavjee, A. S. Slutsky, M. Liu, *Physiol. Genomics* **2004**, *19*, 331.
[50] O. Silbert, Y. Wang, B. S. Maciejewski, H. Lee, S. K. Shaw, J. Sanchez–Esteban, *Exp. Lung Res.* **2008**, *34*, 663.
[51] J. A. Gutierrez, R. F. Gonzalez, L. G. Dobbs, *Am. J. Physiol.* **1998**, *274*, L196.
[52] J. Xu, M. Liu, M. Post, *Am. J. Physiol.* **1999**, *276*, L728.
[53] S. P. Arold, E. Bartolák-Suki, B. Suki, *Am. J. Physiol. Cell. Mol. Physiol.* **2009**, *296*, L574.
[54] J. Sanchez-Esteban, L. a Cicchiello, Y. Wang, S.-W. Tsai, L. K. Williams, J. S. Torday, L. P. Rubin, *J. Appl. Physiol.* **2001**, *91*, 589.
[55] H. R. Wirtz, L. G. Dobbs, *Science* **1990**, *250*, 1266.
[56] J. Sanchez-Esteban, S.-W. Tsai, J. Sang, J. Qin, J. S. Torday, L. P. Rubin, *Am. J. Med. Sci.* **1998**, *316*, 200.
[57] J. E. Scott, S.-Y. Yang, E. Stanik, J. E. Anderson, *Am. J. Respir. Cell Mol. Biol.* **1993**, *8*, 258.
[58] I. B. Copland, M. Post, *J. Cell. Physiol.* **2007**, *210*, 133.
[59] T. Nakamura, M. Liu, E. Mourgeon, A. Slutsky, M. Post, *Am. J. Physiol. Cell. Mol. Physiol.* **2000**, *278*, L974.
[60] A. O. Stucki, J. D. Stucki, S. R. R. Hall, M. Felder, Y. Mermoud, R. A. Schmid, T. Geiser, O. T. Guenat, *Lab Chip* **2015**, *15*, 1302.
[61] Y. S. Edwards, L. M. Sutherland, J. H. . Power, T. E. Nicholas, A. W. Murray, *FEBS Lett.* **1999**, *448*, 127.
[62] S. Hammerschmidt, H. Kuhn, T. Grasenack, C. Gessner, H. Wirtz, *Am. J. Respir. Cell Mol. Biol.* **2004**, *30*, 396.
[63] N. E. Vlahakis, M. A. Schroeder, A. H. Limper, R. D. Hubmayr, *Am. J. Physiol. Cell. Mol. Physiol.* **1999**, *277*, L167.
[64] S. Ghadiali, Y. Huang, *Crit. Rev. Biomed. Eng.* **2011**, *39*, 297.
[65] B. Suki, D. Stamenović, In *Comprehensive Physiology*; John Wiley & Sons, Inc.: Hoboken, NJ, USA, 2011; Vol. 1, pp. 1317–1351.
[66] M. Liu, A. K. Tanswell, M. Post, *Am. J. Physiol. Cell. Mol. Physiol.* **1999**, *277*, L667.
[67] H.-R. Paur, F. R. Cassee, J. Teeguarden, H. Fissan, S. Diabate, M. Aufderheide, W. G. Kreyling, O. Hänninen, G. Kasper, M. Riediker, B. Rothen-Rutishauser, O. Schmid, *J. Aerosol Sci.* **2011**, *42*, 668.
[68] O. Schmid, F. R. Cassee, *Part. Fibre Toxicol.* **2017**, *14*, 52.
[69] A. Lenz, E. Karg, B. Lentner, V. Dittrich, C. Brandenberger, B. Rothen-Rutishauser, H. Schulz, G. A. Ferron, O. Schmid, *Part. Fibre Toxicol.* **2009**, *6*, 32.
[70] B. M. Rothen-Rutishauser, S. G. Kiama, P. Gehr, *Am. J. Respir. Cell Mol. Biol.* **2005**, *32*, 281.
[71] S. J. M. Skinner, *Adv. Fetal Physiol.* **1989**, *8*, 133.
[72] M. Liu, S. J. Skinner, J. Xu, R. N. Han, A. K. Tanswell, M. Post, *Am. J. Physiol. Cell. Mol. Physiol.* **1992**, *263*, L376.
[73] M. Liu, S. Montazeri, T. Jedlovsky, R. van Wert, J. Zhang, R.-K. Li, J. Yan, *Vitr. Cell. Dev. Biol. - Anim.* **1999**, *35*, 87.
[74] S. J. M. Skinner, C. E. Somervell, D. M. Olson, *Prostaglandins* **1992**, *43*, 413.
[75] D. J. Tschumperlin, S. S. Margulies, *Am. J. Physiol. - Lung Cell. Mol. Physiol.* **1998**, *275*, L1173.
[76] C. M. Waters, K. M. Ridge, G. Sunio, K. Venetsanou, J. I. Sznajder, *J. Appl. Physiol.* **1999**, *87*, 715.
[77] F. Rose, K. Zwick, H. A. GHOFRANI, U. SIBELIUS, W. SEEGER, D. WALMRATH, F. GRIMMINGER, *Am. J. Respir. Crit. Care Med.* **1999**, *160*, 846.
[78] D. J. Tschumperlin, J. Oswari, A. S. S. Margulies, *Am. J. Respir. Crit. Care Med.* **2000**, *162*, 357.
[79] S. Ito, B. Suki, H. Kume, Y. Numaguchi, M. Ishii, M. Iwaki, M. Kondo, K. Naruse, Y. Hasegawa, M. Sokabe,

Am. J. Respir. Cell Mol. Biol. **2010**, *43*, 26.
[80] S. Ito, H. Kume, K. Naruse, M. Kondo, N. Takeda, S. Iwata, Y. Hasegawa, M. Sokabe, *Am. J. Respir. Cell Mol. Biol.* **2008**, *38*, 407.
[81] A. Bergner, M. J. Sanderson, *Am. J. Physiol. Cell. Mol. Physiol.* **2002**, *283*, L1271.
[82] F. E. Uhl, S. Vierkotten, D. E. Wagner, G. Burgstaller, R. Costa, I. Koch, M. Lindner, S. Meiners, O. Eickelberg, M. Königshoff, *Eur. Respir. J.* **2015**, *46*, 1150.
[83] C. Dassow, L. Wiechert, C. Martin, S. Schumann, G. Müller-Newen, O. Pack, J. Guttmann, W. A. Wall, S. Uhlig, *J. Appl. Physiol.* **2010**, *108*, 713.
[84] A. R. Froese, C. Shimbori, P. S. Bellaye, M. Inman, S. Obex, S. Fatima, G. Jenkins, J. Gauldie, K. Ask, M. Kolb, *Am. J. Respir. Crit. Care Med.* **2016**, *194*, 84.
[85] A.-G. Lenz, E. Karg, E. Brendel, H. Hinze-Heyn, K. L. Maier, O. Eickelberg, T. Stoeger, O. Schmid, *Biomed Res. Int.* **2013**, *2013*, 1.
[86] A.-G. Lenz, T. Stoeger, D. Cei, M. Schmidmeir, N. Semren, G. Burgstaller, B. Lentner, O. Eickelberg, S. Meiners, O. Schmid, *Am. J. Respir. Cell Mol. Biol.* **2014**, *51*, 526.
[87] D. T. Butcher, T. Alliston, V. M. Weaver, *Nat. Rev. Cancer* **2009**, *9*, 108.
[88] R. Pörtner, S. Nagel-Heyer, C. Goepfert, P. Adamietz, N. M. Meenen, *J. Biosci. Bioeng.* **2005**, *100*, 235.
[89] B. J. Lawrence, M. Devarapalli, S. V. Madihally, *Biotechnol. Bioeng.* **2009**, *102*, 935.
[90] H.-C. Chen, Y.-C. Hu, *Biotechnol. Lett.* **2006**, *28*, 1415.
[91] D. Cei, Development of a dynamic model of the alveolar interface for the study of aerosol deposition (Ph.D. Thesis), University of Pisa, 2015.
[92] D. Huh, G. A. Hamilton, D. E. Ingber, *Trends Cell Biol.* **2011**, *21*, 745.
[93] D. D. Nalayanda, C. Puleo, W. B. Fulton, L. M. Sharpe, T.-H. Wang, F. Abdullah, *Biomed. Microdevices* **2009**, *11*, 1081.
[94] D. Huh, B. D. Matthews, A. Mammoto, M. Montoya-Zavala, H. Y. Hsin, D. E. Ingber, *Science (80-.).* **2010**, *328*, 1662.
[95] A. Jain, R. Barrile, A. van der Meer, A. Mammoto, T. Mammoto, K. De Ceunynck, O. Aisiku, M. Otieno, C. Louden, G. Hamilton, R. Flaumenhaft, D. Ingber, *Clin. Pharmacol. Ther.* **2018**, *103*, 332.
[96] N. Campillo, I. Jorba, L. Schaedel, B. Casals, D. Gozal, R. Farré, I. Almendros, D. Navajas, *Front. Physiol.* **2016**, *7*, 1.
[97] J. P. Vande Geest, E. S. Di Martino, D. A. Vorp, *J. Biomech.* **2004**, *37*, 1923.
[98] Y. Mermoud, M. Felder, J. D. Stucki, A. O. Stucki, O. T. Guenat, *Sensors Actuators B Chem.* **2018**, *255*, 3647.
[99] J. D. Stucki, N. Hobi, A. Galimov, A. O. Stucki, N. Schneider-Daum, C.-M. Lehr, H. Huwer, M. Frick, M. Funke-Chambour, T. Geiser, O. T. Guenat, *Sci. Rep.* **2018**, *8*, 14359.
[100] M. Felder, B. Trueeb, A. O. Stucki, S. Borcard, J. D. Stucki, B. Schnyder, T. Geiser, O. T. Guenat, *Front. Bioeng. Biotechnol.* **2019**, *7*, 1.
[101] Z. Wang, A. A. Volinsky, N. D. Gallant, *J. Appl. Polym. Sci.* **2014**, *131*, n/a.
[102] E. Berthier, E. W. K. Young, D. Beebe, *Lab Chip* **2012**, *12*, 1224.
[103] K. J. Regehr, M. Domenech, J. T. Koepsel, K. C. Carver, S. J. Ellison-Zelski, W. L. Murphy, L. A. Schuler, E. T. Alarid, D. J. Beebe, *Lab Chip* **2009**, *9*, 2132.
[104] M. W. Toepke, D. J. Beebe, *Lab Chip* **2006**, *6*, 1484.
[105] A. Cipitria, A. Skelton, T. R. Dargaville, P. D. Dalton, D. W. Hutmacher, *J. Mater. Chem.* **2011**, *21*, 9419.
[106] Y. Pan, X. Zhou, Y. Wei, Q. Zhang, T. Wang, M. Zhu, W. Li, R. Huang, R. Liu, J. Chen, G. Fan, K. Wang, D. Kong, Q. Zhao, *Sci. Rep.* **2017**, *7*, 3615.
[107] J. Han, P. Lazarovici, C. Pomerantz, X. Chen, Y. Wei, P. I. Lelkes, *Biomacromolecules* **2011**, *12*, 399.
[108] H. S. Yoo, T. G. Kim, T. G. Park, *Adv. Drug Deliv. Rev.* **2009**, *61*, 1033.
[109] S. Chung, N. P. Ingle, G. A. Montero, S. H. Kim, M. W. King, *Acta Biomater.* **2010**, *6*, 1958.
[110] U. Hersel, C. Dahmen, H. Kessler, *Biomaterials* **2003**, *24*, 4385.
[111] S. Sano, K. Kato, Y. Ikada, *Biomaterials* **1993**, *14*, 817.
[112] R. Vasita, G. Mani, C. M. Agrawal, D. S. Katti, *Polymer (Guildf).* **2010**, *51*, 3706.
[113] A. Khademhosseini, R. Langer, *Biomaterials* **2007**, *28*, 5087.
[114] M. Mader, V. Jérôme, R. Freitag, S. Agarwal, A. Greiner, *Biomacromolecules* **2018**, *19*, 1663.
[115] C. J. E. Wahlund, A. Eklund, J. Grunewald, S. Gabrielsson, *Front. Cell Dev. Biol.* **2017**, *5*.
[116] Y. Lee, S. EL Andaloussi, M. J. A. Wood, *Hum. Mol. Genet.* **2012**, *21*, R125.
[117] M. Mulder, *Basic Principles of Membrane Technology*; Springer Netherlands: Dordrecht, 1996.
[118] J.-M. Anaya, Y. Shoenfeld, A. Rojas-Villarraga, R. A. Levy, R. Cervera, *Autoimmunity: From Bench to Bedside*; El Rosario University Press, 2013.

[119] M. P. Tibbe, A. D. van der Meer, A. van den Berg, D. Stamatialis, L. I. Segerink, In *Biomedical Membranes and (Bio)Artificial Organs*; WORLD SCIENTIFIC, 2018; pp. 295–321.
[120] Y. Shao, J. Fu, *Adv. Mater.* **2014**, *26*, 1494.
[121] T. Pasman, D. W. Grijpma, D. F. Stamatialis, A. A. Poot, *Polym. Adv. Technol.* **2017**, *28*, 1258.
[122] P. Sofokleous, M. H. W. Chin, R. Day, In *Functional 3D Tissue Engineering Scaffolds*; Elsevier, 2018; pp. 101–126.
[123] G. Toskas, S. Heinemann, C. Heinemann, C. Cherif, R.-D. Hund, V. Roussis, T. Hanke, *Carbohydr. Polym.* **2012**, *89*, 997.
[124] W. Sun, G. Chen, F. Wang, Y. Qin, Z. Wang, J. Nie, G. Ma, *Carbohydr. Polym.* **2018**, *181*, 183.
[125] K. M. Z. Hossain, R. M. Felfel, P. S. Ogbilikana, D. Thakker, D. M. Grant, C. A. Scotchford, I. Ahmed, *Macromol. Mater. Eng.* **2018**, *303*, 1700628.
[126] H. Li, Y. Xu, H. Xu, J. Chang, *J. Mater. Chem. B* **2014**, *2*, 5492.
[127] V. Beachley, X. Wen, *Prog. Polym. Sci.* **2010**, *35*, 868.
[128] U. G. T. M. Sampath, Y. C. Ching, C. H. Chuah, J. J. Sabariah, P. C. Lin, *Materials (Basel).* **2016**, *9*, 1.
[129] V. Raeisdasteh Hokmabad, S. Davaran, A. Ramazani, R. Salehi, *J. Biomater. Sci. Polym. Ed.* **2017**, *28*, 1797.
[130] S. Zhang, *Nat. Biotechnol.* **2003**, *21*, 1171.
[131] D. Puppi, X. Zhang, L. Yang, F. Chiellini, X. Sun, E. Chiellini, *J. Biomed. Mater. Res. - Part B Appl. Biomater.* **2014**, *102*, 1562.
[132] S. Agarwal, J. H. Wendorff, A. Greiner, *Adv. Mater.* **2009**, *21*, 3343.
[133] N. Bhardwaj, S. C. Kundu, *Biotechnol. Adv.* **2010**, *28*, 325.
[134] J. Nam, Y. Huang, S. Agarwal, J. Lannutti, *Tissue Eng.* **2007**, *13*, 2249.
[135] B. M. Baker, R. P. Shah, A. M. Silverstein, J. L. Esterhai, J. A. Burdick, R. L. Mauck, *Proc. Natl. Acad. Sci.* **2012**, *109*, 14176.
[136] B. Sun, Y.-Z. Long, F. Yu, M.-M. Li, H.-D. Zhang, W.-J. Li, T.-X. Xu, *Nanoscale* **2012**, *4*, 2134.
[137] M. S. Kim, G. H. Kim, *Mater. Lett.* **2014**, *120*, 246.
[138] A. Schneider, X. Y. Wang, D. L. Kaplan, J. A. Garlick, C. Egles, *Acta Biomater.* **2009**, *5*, 2570.
[139] M. B. Taskin, R. Xu, H. Gregersen, J. V. Nygaard, F. Besenbacher, M. Chen, *ACS Appl. Mater. Interfaces* **2016**, *8*, 15864.
[140] S. Fleischer, R. Feiner, A. Shapira, J. Ji, X. Sui, H. Daniel Wagner, T. Dvir, *Biomaterials* **2013**, *34*, 8599.
[141] L. Horvath, Y. Umehara, C. Jud, F. Blank, A. Petri-Fink, B. Rothen-Rutishauser, L. Horváth, Y. Umehara, C. Jud, F. Blank, A. Petri-Fink, B. Rothen-Rutishauser, *Sci. Rep.* **2015**, *5*, 7974.
[142] J. Berg, T. Hiller, M. S. Kissner, T. H. Qazi, G. N. Duda, A. C. Hocke, S. Hippenstiel, L. Elomaa, M. Weinhart, C. Fahrenson, J. Kurreck, *Sci. Rep.* **2018**, *8*, 1.
[143] C. Mandrycky, Z. Wang, K. Kim, D. Kim, *Biotechnol. Adv.* **2016**, *34*, 422.
[144] S. Derakhshanfar, R. Mbeleck, K. Xu, X. Zhang, W. Zhong, M. Xing, *Bioact. Mater.* **2018**, *3*, 144.
[145] V. K. Vendra, L. Wu, S. Krishnan, In *Nanotechnologies for the Life Sciences*; Wiley-VCH Verlag GmbH & Co. KGaA: Weinheim, Germany, 2011; Vol. 5.
[146] B. Dhandayuthapani, Y. Yoshida, T. Maekawa, D. S. Kumar, *Int. J. Polym. Sci.* **2011**, *2011*.
[147] G. E. Morris, J. C. Bridge, L. A. Brace, A. J. Knox, J. W. Aylott, C. E. Brightling, A. M. Ghaemmaghami, F. R. A. J. A. J. Rose, *Biofabrication* **2014**, *6*, 035014.
[148] H. Harrington, P. Cato, F. Salazar, M. Wilkinson, A. Knox, J. W. Haycock, F. Rose, J. W. Aylott, A. M. Ghaemmaghami, *Mol. Pharm.* **2014**, *11*, 2082.
[149] J. A. Ray, N. Doddi, D. Regula, J. A. Williams, A. Melveger, *Surg. Gynecol. Obstet.* **1981**, *153*, 497.
[150] S. A. Sell, M. J. McClure, C. P. Barnes, D. C. Knapp, B. H. Walpoth, D. G. Simpson, G. L. Bowlin, *Biomed. Mater.* **2006**, *1*, 72.
[151] V. Thomas, X. Zhang, Y. K. Vohra, *Biotechnol. Bioeng.* **2009**, *104*, 1025.
[152] R. Shi, J. Xue, H. Wang, R. Wang, M. Gong, D. Chen, L. Zhang, W. Tian, *J. Mater. Chem. B Mater. Biol. Med.* **2015**, *3*, 4063.
[153] I. J. Hall Barrientos, E. Paladino, P. Szabó, S. Brozio, P. J. Hall, C. I. Oseghale, M. K. Passarelli, S. J. Moug, R. A. Black, C. G. Wilson, R. Zelkó, D. A. Lamprou, *Int. J. Pharm.* **2017**, *531*, 67.
[154] S. K. Nemani, R. K. Annavarapu, B. Mohammadian, A. Raiyan, J. Heil, M. A. Haque, A. Abdelaal, H. Sojoudi, *Adv. Mater. Interfaces* **2018**, 1801247.
[155] A. J. García, M. D. Vega, D. Boettiger, *Mol. Biol. Cell* **1999**, *10*, 785.
[156] M. Rabe, D. Verdes, S. Seeger, *Adv. Colloid Interface Sci.* **2011**, *162*, 87.
[157] X. Wang, B. Ding, B. Li, *Mater. Today* **2013**, *16*, 229.
[158] N. Reddy, R. Reddy, Q. Jiang, *Trends Biotechnol.* **2015**, *33*, 362.

[159] N. Higuita-Castro, M. T. Nelson, V. Shukla, P. A. Agudelo-Garcia, W. Zhang, S. M. Duarte-Sanmiguel, J. A. Englert, J. J. Lannutti, D. J. Hansford, S. N. Ghadiali, *Sci. Rep.* **2017**, *7*, 11623.
[160] W. Fu, Z. Liu, B. Feng, R. Hu, X. He, H. Wang, M. Yin, H. Huang, H. Zhang, W. Wang, *Int. J. Nanomedicine* **2014**, 2335.
[161] M. P. Lutolf, J. A. Hubbell, *Nat. Biotechnol.* **2005**, *23*, 47.
[162] A. Shekaran, A. J. Garcia, *Biochim. Biophys. Acta - Gen. Subj.* **2011**, *1810*, 350.
[163] X. Ren, Y. Feng, J. Guo, H. Wang, Q. Li, J. Yang, X. Hao, J. Lv, N. Ma, W. Li, *Chem. Soc. Rev.* **2015**, *44*, 5680.
[164] J. R. J. Paletta, S. Bockelmann, A. Walz, C. Theisen, J. H. Wendorff, A. Greiner, S. Fuchs-Winkelmann, M. D. Schofer, *J. Mater. Sci. Mater. Med.* **2010**, *21*, 1363.
[165] J. Li, M. Ding, Q. Fu, H. Tan, X. Xie, Y. Zhong, *J. Mater. Sci. Mater. Med.* **2008**, *19*, 2595.
[166] D. Grafahrend, K.-H. Heffels, M. V. Beer, P. Gasteier, M. Möller, G. Boehm, P. D. Dalton, J. Groll, *Nat. Mater.* **2011**, *10*, 67.
[167] A. Rossi, L. Wistlich, K.-H. Heffels, H. Walles, J. Groll, *Adv. Healthc. Mater.* **2016**, *5*, 1939.
[168] L. Wistlich, J. Kums, A. Rossi, K.-H. Heffels, H. Wajant, J. Groll, *Adv. Funct. Mater.* **2017**, *27*, 1702903.
[169] D. E. Wagner, N. R. Bonenfant, D. Sokocevic, M. J. DeSarno, Z. D. Borg, C. S. Parsons, E. M. Brooks, J. J. Platz, Z. I. Khalpey, D. M. Hoganson, B. Deng, Y. W. Lam, R. A. Oldinski, T. Ashikaga, D. J. Weiss, *Biomaterials* **2014**, *35*, 2664.
[170] M. M. De Santis, D. A. Bölükbas, S. Lindstedt, D. E. Wagner, *Eur. Respir. J.* **2018**, 1601355.
[171] B. M. Young, K. Shankar, B. P. Allen, R. A. Pouliot, M. B. Schneck, N. S. Mikhaiel, R. L. Heise, *ACS Biomater. Sci. Eng.* **2017**, *3*, 3480.
[172] C. Monteiller, L. Tran, W. MacNee, S. Faux, A. Jones, B. Miller, K. Donaldson, *Occup. Environ. Med.* **2007**, *64*, 609.
[173] A. Martin, A. Sarkar, *Nanotoxicology* **2017**, *11*, 1.
[174] O. Schmid, C. Jud, Y. Umehara, D. Mueller, A. Bucholski, F. Gruber, O. Denk, R. Egle, A. Petri-Fink, B. Rothen-Rutishauser, *J. Aerosol Med. Pulm. Drug Deliv.* **2017**, *30*, 411.
[175] J.-P. Ng-Blichfeldt, A. Schrik, R. K. Kortekaas, J. A. Noordhoek, I. H. Heijink, P. S. Hiemstra, J. Stolk, M. Königshoff, R. Gosens, *EBioMedicine* **2018**, *36*, 461.
[176] B. R. Dye, D. R. Hill, M. A. H. Ferguson, Y. Tsai, M. S. Nagy, R. Dyal, J. M. Wells, C. N. Mayhew, R. Nattiv, O. D. Klein, E. S. White, G. H. Deutsch, J. R. Spence, *Elife* **2015**, *4*, e05098.
[177] M. Henjakovic, K. Sewald, S. Switalla, D. Kaiser, M. Müller, T. Z. Veres, C. Martin, S. Uhlig, N. Krug, A. Braun, *Toxicol. Appl. Pharmacol.* **2008**, *231*, 68.
[178] P. Delmotte, M. J. Sanderson, *Am. J. Respir. Cell Mol. Biol.* **2006**, *35*, 110.
[179] M. R. Lyons-Cohen, S. Y. Thomas, D. N. Cook, H. Nakano, *J. Vis. Exp.* **2017**, 1.
[180] H. N. Alsafadi, C. A. Staab-Weijnitz, M. Lehmann, M. Lindner, B. Peschel, M. Königshoff, D. E. Wagner, *Am. J. Physiol. - Lung Cell. Mol. Physiol.* **2017**, *312*, L896.
[181] B. Zhang, M. Radisic, *Lab Chip* **2017**, *17*, 2395.
[182] H. Kamble, M. J. Barton, M. Jun, S. Park, N. T. Nguyen, *Lab Chip* **2016**, *16*, 3193.
[183] P. Hamerli, *Biomaterials* **2003**, *24*, 3989.
[184] K. L. Sellgren, E. J. Butala, B. P. Gilmour, S. H. Randell, S. Grego, *Lab Chip* **2014**, *14*, 3349.
[185] S. Sharma, S. Mohanty, D. Gupta, M. Jassal, A. K. Agrawal, R. Tandon, *Mol. Vis.* **2011**, *17*, 2898.
[186] A. Elamparithi, A. M. Punnoose, S. Kuruvilla, M. Ravi, S. Rao, S. F. D. Paul, *Artif. Cells, Nanomedicine Biotechnol.* **2016**, *44*, 878.
[187] K. Wang, X. Chen, Y. Pan, Y. Cui, X. Zhou, D. Kong, Q. Zhao, *Biomed Res. Int.* **2015**, *2015*, 1.
[188] S. G. Wise, M. J. Byrom, A. Waterhouse, P. G. Bannon, M. K. C. Ng, A. S. Weiss, *Acta Biomater.* **2011**, *7*, 295.
[189] C. P. Laurent, C. Vaquette, X. Liu, J.-F. Schmitt, R. Rahouadj, *J. Biomater. Appl.* **2018**, *32*, 1276.
[190] Y. ZHU, M. LEONG, W. ONG, M. CHANPARK, K. CHIAN, *Biomaterials* **2007**, *28*, 861.
[191] F. Pati, T.-H. Song, G. Rijal, J. Jang, S. W. Kim, D.-W. Cho, *Biomaterials* **2015**, *37*, 230.
[192] J. Liao, X. Guo, K. J. Grande-Allen, F. K. Kasper, A. G. Mikos, *Biomaterials* **2010**, *31*, 8911.
[193] E. Lih, K. W. Park, S. Y. Chun, H. Kim, T. G. Kwon, Y. K. Joung, D. K. Han, *ACS Appl. Mater. Interfaces* **2016**, *8*, 21145.
[194] A. Burgess, K. Shah, O. Hough, K. Hynynen, *Expert Rev. Neurother.* **2015**, *15*, 477.
[195] K. Wang, M. Zhu, T. Li, W. Zheng, L. Li, M. Xu, Q. Zhao, D. Kong, L. Wang, *J. Biomed. Nanotechnol.* **2014**, *10*, 1588.
[196] J. Groll, J. A. Burdick, D. Cho, B. Derby, M. Gelinsky, S. C. Heilshorn, T. Jüngst, J. Malda, V. A. Mironov,

K. Nakayama, A. Ovsianikov, W. Sun, S. Takeuchi, J. J. Yoo, T. B. F. Woodfield, *Biofabrication* **2018**, *11*, 013001.
[197] L. Moroni, T. Boland, J. A. Burdick, C. De Maria, B. Derby, G. Forgacs, J. Groll, Q. Li, J. Malda, V. A. Mironov, C. Mota, M. Nakamura, W. Shu, S. Takeuchi, T. B. F. Woodfield, T. Xu, J. J. Yoo, G. Vozzi, *Trends Biotechnol.* **2018**, *36*, 384.
[198] J. Malda, J. Visser, F. P. Melchels, T. Jüngst, W. E. Hennink, W. J. A. Dhert, J. Groll, D. W. Hutmacher, *Adv. Mater.* **2013**, *25*, 5011.
[199] T. Jungst, W. Smolan, K. Schacht, T. Scheibel, J. Groll, *Chem. Rev.* **2016**, *116*, 1496.
[200] E. Correa-Meyer, L. Pesce, C. Guerrero, J. I. Sznajder, *Am. J. Physiol. Cell. Mol. Physiol.* **2002**, *282*, L883.
[201] K. J. Cavanaugh, T. S. Cohen, S. S. Margulies, *Am. J. Physiol. Physiol.* **2005**, *290*, C1179.
[202] L. Yang, A. Feuchtinger, W. Möller, Y. Ding, D. Kutschke, G. Möller, J. C. Schittny, G. Burgstaller, W. Hofmann, T. Stoeger, Daniel Razansky, A. Walch, O. Schmid, *ACS Nano* **2019**, acsnano.8b07524.
[203] E. R. Weibel, In *Comprehensive Physiology*; John Wiley & Sons, Inc.: Hoboken, NJ, USA, 2011.
[204] S. Hammerschmidt, H. Kuhn, T. Grasenack, C. Gessner, H. Wirtz, *Am. J. Respir. Cell Mol. Biol.* **2004**, *30*, 396.
[205] J. Sanchez-esteban, Y. Wang, E. J. Filardo, L. P. Rubin, D. E. Ingber, Y. Wang, E. J. Filardo, L. P. Rubin, D. E. I. Integrins, **2006**, *02905*, 343.
[206] S. P. Arold, J. Y. Wong, B. Suki, *Ann. Biomed. Eng.* **2007**, *35*, 1156.
[207] N. J. Douville, P. Zamankhan, Y.-C. Tung, R. Li, B. L. Vaughan, C.-F. Tai, J. White, P. J. Christensen, J. B. Grotberg, S. Takayama, *Lab Chip* **2011**, *11*, 609.
[208] Z. Huang, Y. Wang, P. S. Nayak, C. E. Dammann, J. Sanchez-Esteban, *J. Biol. Chem.* **2012**, *287*, 18091.
[209] Y. Wang, Z. Huang, P. S. Nayak, B. D. Matthews, D. Warburton, W. Shi, J. Sanchez-Esteban, *J. Biol. Chem.* **2013**, *288*, 25646.
[210] J. A. Gilbert, P. S. Weinhold, A. J. Banes, G. W. Link, G. L. Jones, *J. Biomech.* **1994**, *27*, 1169.
[211] J. E. Anderson, E. Yen, R. S. Carvalho, J. E. Scott, *Vitr. Cell. Dev. Biol. - Anim.* **1993**, *29*, 183.
[212] R. Sreenivasan, E. K. Bassett, D. M. Hoganson, J. P. Vacanti, K. K. Gleason, *Biomaterials* **2011**, *32*, 3883.
[213] T. V. Chirila, Z. Barnard, Zainuddin, D. G. Harkin, I. R. Schwab, L. W. Hirst, *Tissue Eng. Part A* **2008**, *14*, 1203.
[214] J. A. Matthews, G. E. Wnek, D. G. Simpson, G. L. Bowlin, *Biomacromolecules* **2002**, *3*, 232.
[215] G. E. Wnek, M. E. Carr, D. G. Simpson, G. L. Bowlin, *Nano Lett.* **2003**, *3*, 213.
[216] A. Nishiguchi, S. Singh, M. Wessling, C. J. Kirkpatrick, M. Möller, *Biomacromolecules* **2017**, *18*, 719.
[217] S. Hinderer, J. Seifert, M. Votteler, N. Shen, J. Rheinlaender, T. E. Schäffer, K. Schenke-Layland, *Biomaterials* **2014**, *35*, 2130.
[218] M. Frydrych, S. Román, S. MacNeil, B. Chen, *Acta Biomater.* **2015**, *18*, 40.
[219] R. M. Aghdam, S. Najarian, S. Shakhesi, S. Khanlari, K. Shaabani, S. Sharifi, *J. Appl. Polym. Sci.* **2012**, *124*, 123.
[220] Y. Qian, L. Li, C. Jiang, W. Xu, Y. Lv, L. Zhong, K. Cai, L. Yang, *Int. J. Biol. Macromol.* **2015**, *79*, 133.
[221] L. Tayebi, M. Rasoulianboroujeni, K. Moharamzadeh, T. K. D. Almela, Z. Cui, H. Ye, *Mater. Sci. Eng. C* **2018**, *84*, 148.

Figures and Captions

Figure 1. Role of (cyclic) mechanical forces in lung epithelium. Proliferation, differentiation, adhesion, migration, and apoptosis of lung epithelial cells are regulated by cyclic stretch. These effects can be initiated by several distinct cellular pathways such as the MAPK/ERK pathway, which results in the differentiation of fetal epithelial cells [45], the cAMP-PKA-dependent signaling pathway mediating differentiation of fetal ATIIs [46], and activation of YAP/TAZ and the signaling cascade of Cdc42/F-actin/MAPK mediating alveolar regeneration [47,48,200]. Cyclic strain induced by ventilation regulates pulmonary epithelial morphology by a pathway involving Src, FAK, and then MAPK/ERK signaling [49]. High deformation opens the tight junctions, disrupts barrier integrity and increases translocation of micromolecules across the alveolar epithelium by activation of intracellular signaling pathways [13,201].

Figure 2. Schematic depictions and photos of *in vitro* epithelial cell culture systems and stretching devices. (a) *In vitro* cell culture model under submerged conditions. (b) *In vitro* static cell culture model under ALI conditions using Transwell® insert. (c) A stretching system using a solenoid unit: Fetal rat lung cell on a Gelfoam sponge fixed to the dish at one end, and another end is stretched using an electromagnetic field [74]. (d) A cell-stretching device to apply a uniform, equibiaxial strain to the cells: The membrane deformed by moving the indentor to provide an equibiaxial strain [75]. (e) Commercial Flexcell Strain Unit™ (Flexcell International Corporation): This device applies uniaxial radial strain by regulating vacuum pressure underneath a flexible silicone membrane. (f) The MALI bioreactor system: The system is composed of a basal and an apical chamber separated by a stretchable, porous membrane and two fluidic systems for cell culture medium. Epithelial cells cultured on a membrane under ALI conditions. A pressure regulator in the apical chamber to actuate the flexible membrane in a controlled manner [91]. (g) (left) A

microfluidic system for co-culture of epithelial and endothelial cells under ALI and mechanical stretch: This microsystem applies a uniaxial strain on a stretchable, porous PDMS membrane by regulating the pressure in the side chambers (right) Image of a side and tope view of an actual microfluidic, reproduced with permission [94] Copyright 2010, American Association for the Advancement of Science (h) (top) A lung-on-a-chip array: The membrane is stretched in a tri-axial direction using pneumatic microchannels located at the bottom of the basolateral chamber [60]. (down) Photograph of a modified lung-on-chip with 6 independent chamber, reproduced under the terms of the a Creative Commons Attribution 4.0 International License [99]. Copyright 2018, Springer Nature.

Figure 3. Lung morphology and cellular structure as guidance for bioinspired lung models. (a) A 3D reconstruction of the entire *murine* lung tissue obtained with Light Sheet Fluorescence Microscopy (LSFM) depicting trachea, bronchi, small (terminal) bronchioles (I), distal bronchial tree (II) (reproduced with permission from [202]; Copyright (2019) American Chemical Society), and 3D honeycomb structure of the alveolar region as observed with confocal microscopy on precision cut lung slices (III) as well as surface rendering (IV) and 2D images thereof (V). Green: tissue structure, blue: nuclei. (b) Schematic of cellular composition of the human airway tree from upper bronchus to alveolus. (c) (left) SEM image of the human alveolar wall showing the very thin tissue barrier separating capillary blood and air (right) TEM image of alveolar-capillary region depicting the alveolar epithelium (EP), capillary endothelium (EN), basement membranes (BM) as part of the air-blood barrier, fibroblast (FB), and erythrocyte (EC) (Electron microscopy images reproduced with permission [35] Copyright 1978, Elsevier and [203] Copyright 2011, John Wiley and Sons). (d) Schematic depiction of characteristics of a state-of-the-art membrane mimicking the alveolar-capillary basement membrane.

Figure 1.

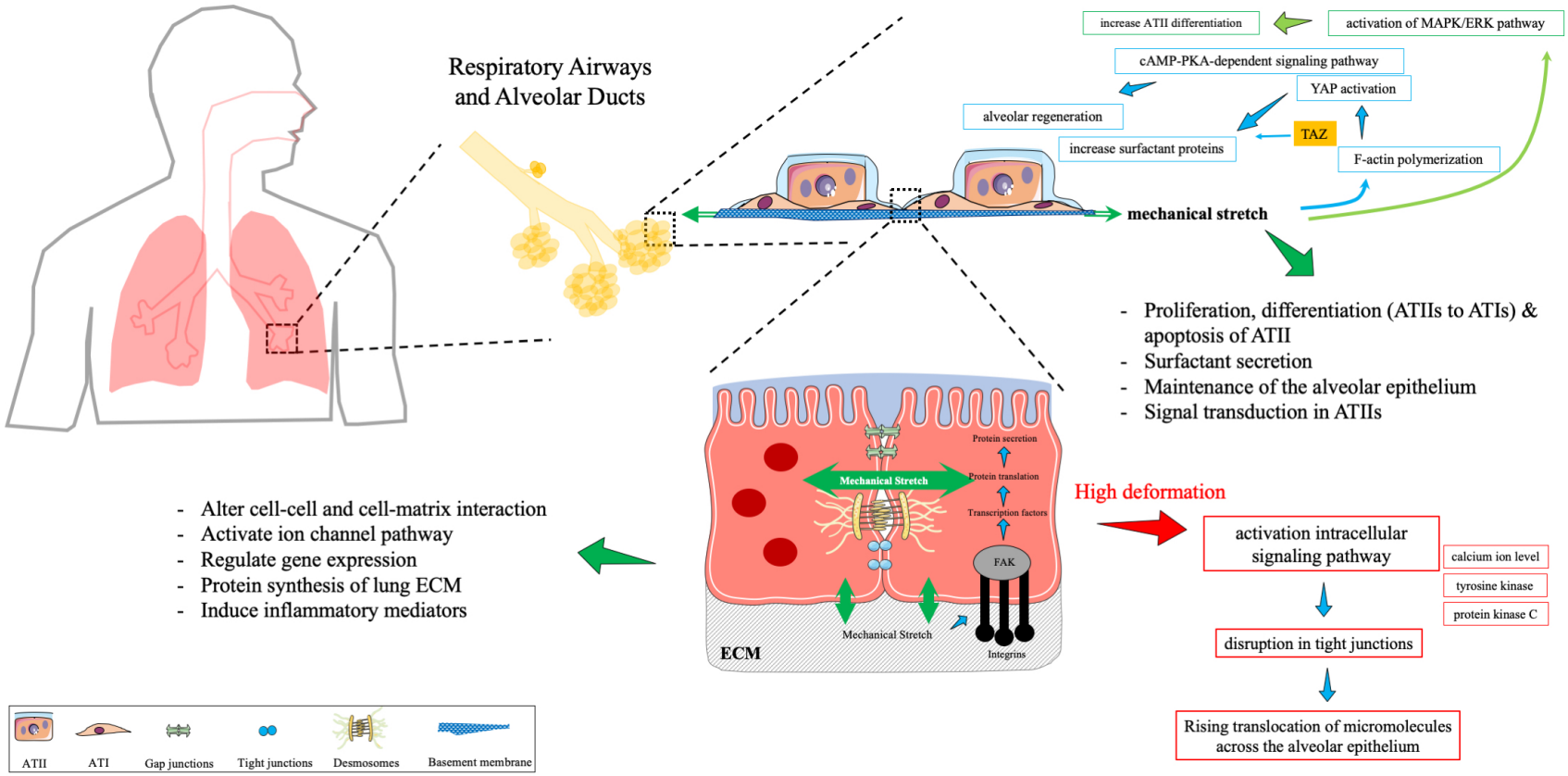
Respiratory Airways
and Alveolar Ducts
increase ATII differentiation
activation of MAPK/ERK pathway
cAMP-PKA-dependent signaling pathway
YAP activation
alveolar regeneration
TAZ
increase surfactant proteins
F-actin polymerization
mechanical stretch
- Proliferation, differentiation (ATIIs to ATIs) & apoptosis of ATII
- Surfactant secretion
- Maintenance of the alveolar epithelium
- Signal transduction in ATIIs
Protein secretion
Protein translation
Transcription factors
Mechanical Stretch
FAK
Mechanical Stretch
Integrins
ECM
High deformation
activation intracellular signaling pathway
calcium ion level
tyrosine kinase
protein kinase C
disruption in tight junctions
Rising translocation of micromolecules across the alveolar epithelium
- Alter cell-cell and cell-matrix interaction
- Activate ion channel pathway
- Regulate gene expression
- Protein synthesis of lung ECM
- Induce inflammatory mediators
ATII
ATI
Gap junctions
Tight junctions
Desmosomes
Basement membrane

Figure 2.

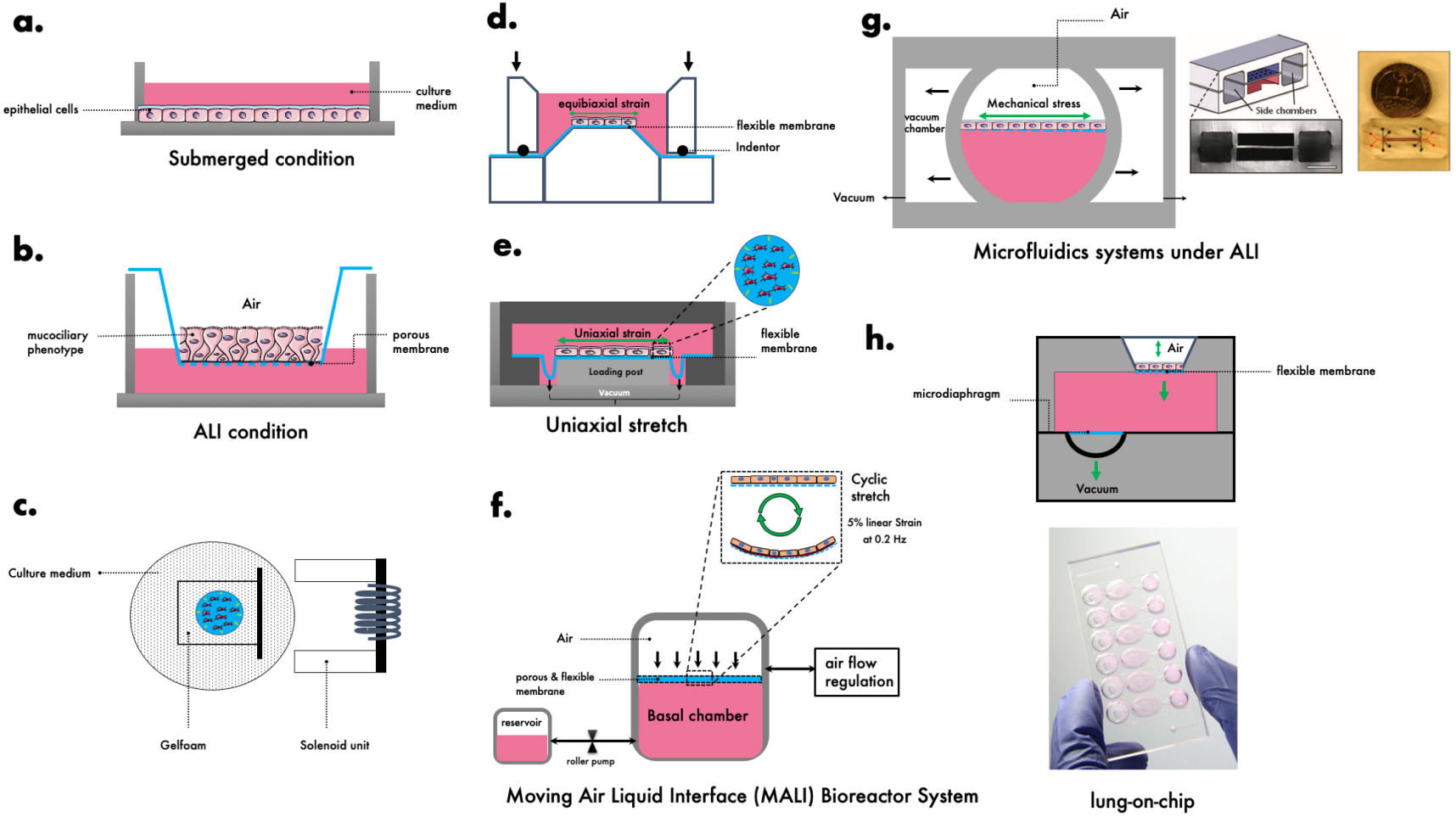
a.
epithelial cells
culture medium
Submerged condition
b.
Air
mucociliary phenotype
porous membrane
ALI condition
c.
Culture medium
Gelfoam
Solenoid unit
d.
equibiaxial strain
flexible membrane
Indentor
e.
Uniaxial strain
flexible membrane
Loading post
Vacuum
Uniaxial stretch
f.
Cyclic stretch
5% linear Strain at 0.2 Hz
Air
porous & flexible membrane
air flow regulation
Basal chamber
reservoir
roller pump
Moving Air Liquid Interface (MALI) Bioreactor System
g.
Air
Mechanical stress
vacuum chamber
Vacuum
Side chambers
Microfluidics systems under ALI
h.
Air
flexible membrane
microdiaphragm
Vacuum
lung-on-chip

Figure 3.

(a) Morphology of whole murine lung tissue

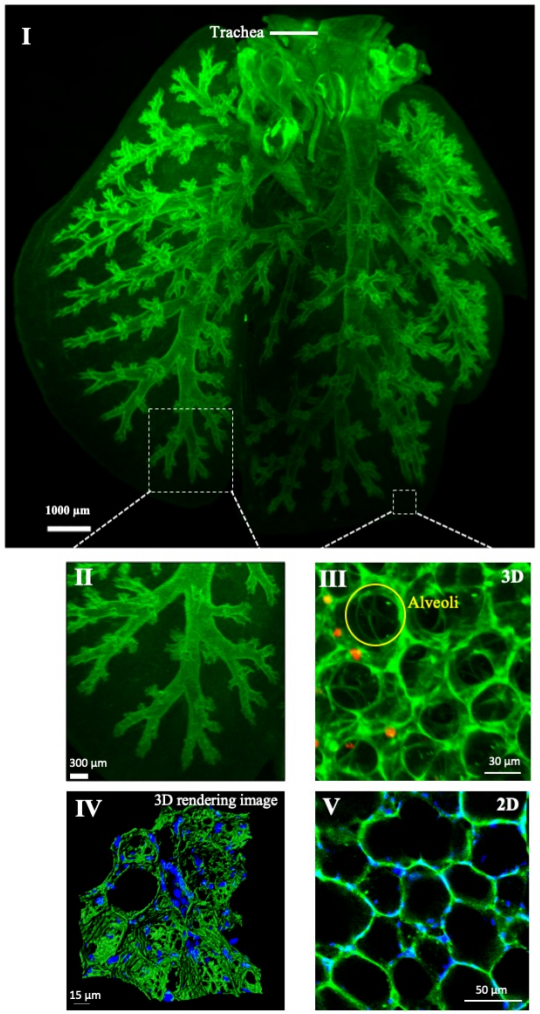

(b) Human airway wall cellular composition

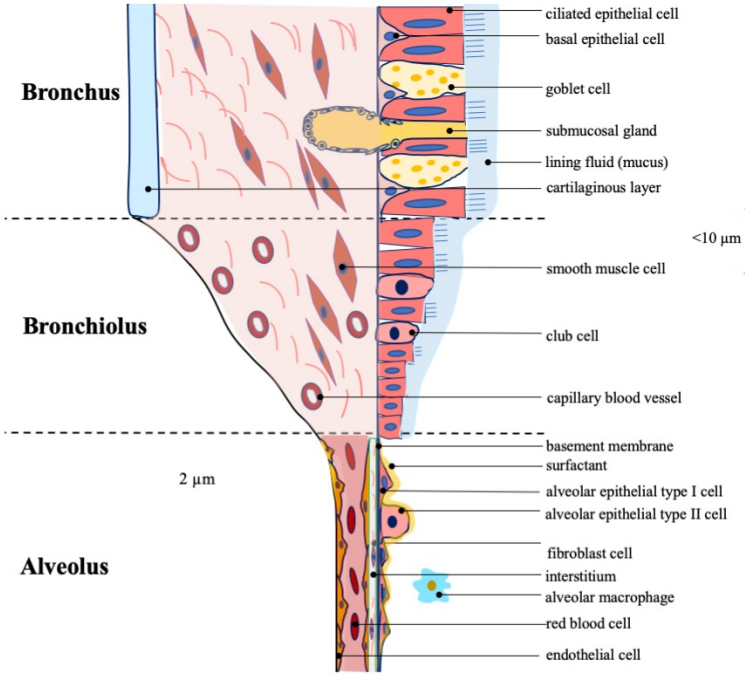

(d) State-of-the-art of the basement membrane

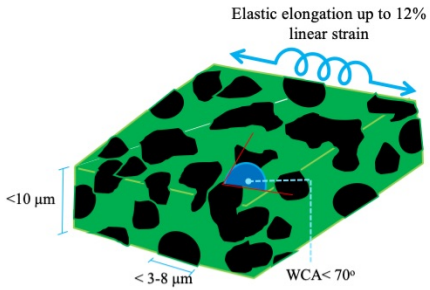

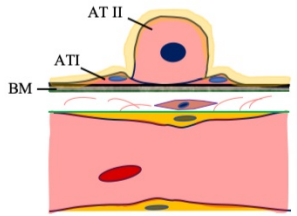

(c) EM of alveolar-capillary region

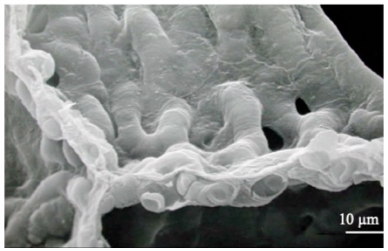

alveolar wall

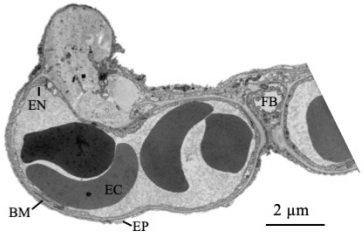

alveolar capillary

Table 1. The stretch- and permeability-related physiologic parameters of the native basement membrane of the human alveolar-capillary tissue

Parameter	Value	References
Level of mechanical linear (1D) strain	4%*[1] –12%*[2] (20%*[3])	[24–28]
Corresponding 2D strain	8%*[1] – 25%*[2] (44%*[3])	
Stiffness of human alveolar tissue	1-2 kPa	[36,37]
Pore diameter of alveolar-capillary barrier	0.5–2.5 nm*[4]	[33]
Thickness of basement membrane	ca. 50 nm	[30]
Thickness of air-blood tissue barrier	0.62 μm ± 0.04*[5]	[30,35]
Total alveolar-capillary barrier thickness	1.1 μm ± 0.1*[5]	[30,34]

*[1] normal breathing, *[2] deep inspiration, heavy exercise, *[3] pathological conditions, *[4] with a small portion of larger pores (< 400 nm) *[5] harmonic mean

Table 2. *In vitro* effects of (cyclic) mechanical forces on epithelial cell physiology of the lung and associated cell stretch-conditions

Mechanical stretch			Cell Stretching Device	Cell type	Key results	Ref.
Type	Level	Frequency (cycles per minute)				
Single	16-17% (surface area)	27	Hydrostatic force unit	rATII	Mechanical stretch of ATIIs caused an increase in cytosolic Ca^{2+} followed by stimulation of surfactant secretion.	[55]
Intermittent	12- 18% (linear)	30	Solenoid stretch unit	fetal rat lung organotypic	Both frequency and amplitude of cyclic stretch affects production of prostacyclin by lung cells.	[74]
Cyclic	10% (surface area)	3 or 50	Flexecell strain unit	fetal rabbit ATII	Mechanical stretch alters ATII proliferation rate and may also affect synthesis of surfactant-related phospholipids.	[57]
Cyclic	27-30% (surface area)	15	Flexcell strain unit	ASMs	Cyclic stretch resulted in proliferation of ASMs and it may contribute to increased ASMs hyperplasia and airway resistance.	[42]
Cyclic	12.5% (max.), Ave. < 5.7% (linear)	60	Solenoid stretch unit/Flexcell Strain Unit	Organotypic epithelial/fibroblasts	Stretch enhanced DNA synthesis of mixed cells, epithelial cells, and fibroblasts in 3D culture conditions.	[10]
Cyclic	12, 24, 37, and 50% (surface area)	15	Stretch Hydrostatic force unit	rATII	Deformation-induced injury is an important factor in the development of lung injury during mechanical ventilation.	[75]
Cyclic	Max. 20-22% (surface area)	10-30	Flexcell strain unit	Calu-3, Cat tracheal epithelial, $1HAEo^-$	Wound healing affected by cyclic mechanical strain and wound closure was inhibited by both strain and compression (decreased ability to repair).	[41]
Static distention	21% (surface area)	-	Hydrostatic force unit	rATII	Mechanical stretch influenced alveolar epithelial phenotypic expression *in vitro*, at least in part, at the transcriptional level (increase in the marker for the type I phenotype (rTI40) and decrease in mRNA content of SFTPB, SFTPC, and no effect on mRNA content of SFTPA or GAPDH.	[51]
Cyclic	5%-15% (radial)	50	Flexcell strain unit	NCI-H441	Cyclic mechanical stretching of H441 cells for 24 hours increased SFTPB and SFTPA expression.	[56]
Cyclic	20-30% (surface)	20 and 40	Flexcell strain unit	A549	High deformation (more than 20%) can activate inflammatory response IL8.	[63]
Cyclic	5% (linear)	60	Solenoid stretch unit	Organotypic epithelial and fibroblasts	Cyclic mechanical strain differentially regulates gene and protein expression of ECM molecules in fetal lung cells.	[52]
Cyclic	Max. 22% (surface area)	3	Flexcell strain unit	rATII	Mechanical stretch can induce both apoptosis and phosphatidylcholine secretion in ATII.	[61]
Cyclic	25%, 37%, and 50% (surface area)	15 and 60	Over-distension injury model	rATII	The frequency of sustained cyclic deformations (not the deformation rate during a single stretch) increased deformation-induced injury.	[78]
Cyclic	5% (linear)	60	Solenoid stretch unit	Organotypic epithelial and fibroblasts	Mechanical strain significantly increased SFTPC and tropoelastin mRNA expression.	[59]

Cyclic	20% (surface area)	60	Flexcell strain unit	NCI-H441	Mechanical stretch induces proliferation of pulmonary epithelial cells. Tyrosine kinase activity is necessary to signal the proliferative response to mechanical strain. Activation of FAK via tyrosine phosphorylation does not appear to have a role in the strain response.	[43]
Cyclic	5% (linear)	50	Flexcell strain unit	fetal ATII	Cyclic mechanical stretch enhances differentiation of fetal ATIIs in mesenchymal-epithelial interactions.	[54]
Cyclic biaxial	Max. 10% (linear)	30	Biaxial stretching device	1HAEo$^-$ and 16HBE14o$^-$	Uniform biaxial elongation inhibits epithelial wound closure.	[39]
Cyclic	5 and 30% (surface area)	30		rATII	Cyclic stretch induces a rapid ERK1/2 activation, which is transduced via G proteins and EGFR tyrosine kinase. Stretch-induced MAPK/ERK pathway activation is independent of Na^+ and Ca^{2+} influxes and the Grb2-SOS, Ras, Raf-1 pathway.	[200]
Cyclic	10 % (surface area)	60	Flexcell strain unit	A549	Cyclic stretch altered the intracellular transport of plasmids to increase gene expression.	[204]
Cyclic	20% (surface area)	30	Flexcell strain unit	A549	Mechanical stretch changed cell morphology of ATII-like A549 and activated Src protein tyrosine kinase.	[49]
Cyclic	5% (linear)	60	Flexcell strain unit	fetal rATII	Mechanical stretch, at least in part, induces differentiation of fetal ATII via EGFR activation of the MAPK/ERK pathway.	[45]
Cyclic	13% and 30% (surface area)	40 and 60	Flexcell strain unit	rATII	Increased mechanical stretch contributes to lung injury by induction of apoptosis and necrosis in ATIIs.	[62]
Cyclic	5% (linear)	60	Flexcell strain unit	E19 fetal ATII	Various integrins contribute to mechanical control of ATII cell differentiation on laminin substrates. Strain-induced differentiation of fetal ATIIs is mediated by specific ECM-integrin interactions.	[205]
Cyclic	5% (linear)	60	Flexcell strain unit	E19 fetal ATII	The transcription factor-dependent protein kinase (cAMP-PKA-dependent) signaling pathway is activated by force in fetal ATIIs and participates in strain-induced fetal ATII cell differentiation.	[46]
Cyclic	Average 10% (max. 20%) (surface area)	20	Flexcell strain unit	NCI-H441, A549	Cyclic mechanical stretch induced by ventilation supports pulmonary epithelial proliferation by a pathway involving Src, FAK, and then MAPK/ERK signaling.	[44]
Cyclic continuous	5, 10, or 17% (radial elongations)	30	Flexcell strain unit	Fetal rATII	Mechanical stretch of fetal ATIIs evokes a complex network of signaling molecules, which diverge downstream to regulate the temporal expression of a unique set of early response genes.	[58]
Cyclic	25, 50, 75 and 100% (surface area)	12	Over-distension injury model	MLE-12	The basement ECM plays a key role in both cell death and signal transduction in response to strain.	[206]
Cyclic	5%, 10%, and 15% (linear)	10–30	Flexcell strain unit	Primary rATII	Different types of mechanical strain inhibited wound closure of ATIIs compared with static controls. Mechanical stretch decreases migration of AT cells through mechanisms involving Tiam1, a Rac1-specific guanine nucleotide exchange factor.	[40]
Cyclic	12.5, 25, or 50% (surface area)	3	Over-distension injury model	rATII	Variable mechanical stretch may enhance surfactant secretion (reducing the risk of ventilator-induced lung injury).	[53]
Cyclic	38% in the latitudinal and up to 44% in the longitudinal direction (linear)	15	Strain-applying bioreactor	PCLS	Stretching of PCLS on PDMS-membranes represents a useful model to investigate lung stretch in intact lung tissue *in vitro* for several hours.	[83]

Cyclic	5-15% (linear)	12	Human alveolar-capillary interface model	A549	Studying the effects of the mechanical strain on inflammatory response by mimicking the lung alveolar-capillary barrier.	[94]
Cyclic	15% (surface area)	52	Flexcell strain unit	Primary murine ATII	Cyclic stretch induces epithelial-mesynchemal transition (EMT) in ATIIs through production of the matrix component hyaluronan which activates the Wnt/beta-catenin pathway downstream of MyD88 signaling.	[14]
Cyclic	15-50% (surface area)	12-18	Microfluidic alveolar model	Murine ATII, A549	Studying the combined effects of surface-tension stresses and cyclic stretch on AT cells	[207]
Cyclic	5% (linear)	40	Flexcell strain unit	Fetal mATII	EGFR and ErbB4 regulate stretch-induced ATIIs differentiation via MAPK/ERK pathway.	[208]
Cyclic	5% (linear)	40	Flexcell strain unit	E19 fetal ATII	Mechanical strain enhances binding of alpha6beta1 integrin to TACE to promote fetal ATIIs differentiation.	[209]
Cyclic	21% (surface area)	12	Alveolar-on-a-chip	16HBE14o, pHPAEC	Investigation of the effect of cyclic stretch on the metabolic activity and the cytokine secretion of pHPAEC using an alveolus-on-a-chip array.	[60]
Cyclic	6% (linear)	60	A chip to partially mimic OSA	rMSCs	HIF-1α expression in rMSCs increases in response to Intermittent hypoxia and mechanical stretch.	[96]

Table 3. Overview of cell stretch devices employed in *in vitro* studies on the effect of mechanical stretch on cell and tissue models of the lung

Type of device (**depicted in Fig. 2 panel C-H**)	Cell culture conditions	Type of stretch		Membrane material				Ref.
		Direction	Max. strain applicable	Material	Pore size	Cell growth area (mm^2)	Thickness (μm)	
Solenoid stretch unit (**C**)	Submerged	1D, uniaxial	18% (linear)	Gelfoam sponge	NP*[1]	14x10	2000	[71,72]
Stretch unit by applying hydrostatic pressure	Submerged	2D, biaxial	50% (surface area)	Silicoelastic	NP	415	230	[55]
Cell stretching device to model over-distension injury (**D**)	Submerged	2D, equibiaxial	50% (surface area)	Silicone	NP	–	200	[75]
Flexcell strain unit (Flexcell International Corp., NC) **(E)**	Submerged	2D, equibiaxial	15% (radial)	Bioflex silicone	NP	420	–	[57,210,211]
Strain-applying bioreactor	*Ex vivo* model	1D, uniaxial	ca. 30% (longitudinally and latitudinally)	PCLS-PDMS	–	–	436 *[2]	[83]
Stretch apparatus (ST-150; Strex, Osaka, Japan)	Submerged	1D, uniaxial	30% (surface area)	Silicone chamber	NP	10x10	–	[79,80]
Human alveolar-capillary interface model (**G**)	ALI	1D, uniaxial	15% (linear)	PDMS	10 μm*[3]	0.028 *[4]	10	[94]
Alveolar-on-a-chip (**H**)	ALI	3D, tri-axial	21% (surface area)	PDMS	3 or 8 μm	2x7.1	3	[60]
A chip to mimic OSA	Submerged	1D, uniaxial	6% (linear)	PDMS	–	12.5 *[5]	10	[96]
MALI bioreactor system (**F**)	ALI	3D, tri-axial	17% (linear)	Bionate® II 80A (PCU)	–	420	75.4	[91]

*[1] Non-porous, *[2] PCLS: 400 μm, PDMS: 33–36 μm, *[3] wide pentagonal, *[4] cross sectional: 400 μm (width) in 70 μm (height), *[5] only diameter of main chamber reported

Table 4. Synthetic and natural- based polymers as candidate materials for stretchable and porous membranes

Type	Material		Manufacturing method	Physical properties				Mechanical properties				Cell type	Ref.
				Water contact angle (°)	Thickness (μm)	Porosity (%)	Pore size /area	Tensile Stress (MPa)	Elastic Modulus (MPa)	Elongation at break (%)	Max. elastic Strain (%)/ Compliance		
Synthetic-based	PCL*[1]		ES	90	30	85	0.2-0.4 μm	1.74	3.55	30.08	NA	HLEC	[185]
	PCL*[2]		ES	NA	NA	52.5	NA	0.032	0.036	129.29	NA	L6 rat myoblasts	[186]
	P(LLA-CL)		Melt spinning	NA	33 and 118*[3]	<85	1-16 μm^2	26.1	23.5	578.2	C: 0.0149 ml mm Hg^{-1} *[4]	3T3 fibroblasts	[109]
	PET		ES	NA	120	83.6	NA	NA	NA	NA	NA	CALU-3 and MRC5	[147]
	PET		ES	NA	60	NA	NA	NA	NA	NA	NA	CALU-3, MRC5 and DCs	[148]
	Silicone/PTFE		iCVD	NA	0.5-3*[5], 20*[6]	Non	0.1 μm*[7]	NA	6.24-9.72	NA	NA	Not Studied	[212]
	Bionate® II 80A (PCU)		ES	121.5	75.4	NA	NA	54.2	2.2	501	NA	A549	[91]
Natural-based	Silk		Casting	NA	10-15	NA	0.5-5μm	NA	NA	NA	NA	HLEC	[213]
	Collagen		ES	NA	187	NA	NA	1.5*[8], 0.7*[9]	52.3*[8], 26.1*[9]	NA	NA	Aortic SMCs	[214]
	Fibrinogen		ES	NA	700	NA	NA	2	80	NA	NA	Not studied	[215]
Blend	PCL/NCO–sP(EO-stat-PO)		ES	NA	10	71	1.5 μm	3.8 *[10]	5.2	430 *[10]	15 *[10]	NCI H441, HUVECs /HPMEC, HPAEC	[216]
	PEGdma/PLA	PLA	ES	131.8	NA	NA	1836 μm^2	2	64.1	275	NA	VECs and VICs	[217]
		Blend	ES	38.7	<50*[10]	NA	8.27 μm^2	2.1	141	4	NA		
	PLLA/Lung dECM		ES	129.2	139±53	86.75	NA	NA	16.35	NA	NA	HBSMCs	[171]
	PGS/PLLA		Freeze-drying	NA	830	92	109–141μm	0.007	0.030	NA	26.17	ADSCs	[218]
	Fibronectin grafted P(LLA-CL)		ES	NA	3000	60.4	1-3 μm	5.2	50*[11]	80	80	PEECs	[190]
	PCL/ rhTE		ES	NA	<100-200	NA	NA	0.510	< 0.3	NA	< 0.007 kPa^{-1}	HUVECs	[188]
	PCL/Gelatin*[12]	PCL	ES	NA	<20	NA	NA	NA	7.20	NA	NA	A549/ HSAEC & HUVECs	[159]
		PCL/Gelatin 75:25	ES	NA	<20	NA	NA	NA	2.10	NA	NA		
		PCL/Gelatin 50:50	ES	NA	<20	NA	NA	NA	0.36	NA	NA		
	PCL/Gelatin*[13]	PCL	ES	130.52	NA	NA	37.6 μm	1.18	4.41	614.90	NA	HUVECs	[187]
		Blend	ES	58.18-70.85*[14]	NA	NA	8-12.4 μm *[14]	0.55-0.76*[14]	3.02-5.85*[14]	551- 742*[14]	NA		
	PDS/Gelatin/ Elastin	PDS	ES	NA	500	80-82	NA	5.61	17.11	216.7	NA	Not studied	[151]
		Blend	ES	NA	500	80-82	NA	1.77	5.74	75.08	NA		
	PCL/PDS	PCL	ES	131.28	NA	NA	~23 μm *[10]	<4*[10]	<1*[10]	<260*[10]	NA	*In vivo* vascular graft	[106]
		PDS	ES	11.54	NA	NA	~18 μm *[10]	<9.5*[10]	<4.2*[10]	<70*[10]	NA		
		Blend	ES	78.06	NA	NA	20.06 μm	<7.1*[10]	<2.5*[10]	121.3	NA		
	PLGA/Gelatin/ Elastin		ES	NA	20-1000	NA	0.6-4.74 μm^2	0.130	0.770	NA	NA	Human EA.hy926& BASMCs	[107]
	PCL/PGA	PCL	ES	118	NA	81.3	1.05 nm	<1.8*[10]	<1.5*[10]	<10*[10]	NA	Not studied	[219]
		PGA	ES	0	NA	90	2.3 nm	<8*[10]	<19*[10]	<105*[10]	NA		
		Blend	ES	54-103	NA	84-87.8	1.3-1.9 nm	<2.5-5.5*[10]	<2-15*[10]	<25-95*[10]	NA		
	PCL/HA	PCL	ES	123	200	NA	NA	4.1	0.68	213	NA	FEK4	[220]
		PCL/HA, 5:1	ES	78	200	NA	NA	10*[10]	0.275*[10]	90*[10]	NA		
		PCL/HA, 5:2	ES	54	200	NA	NA	11*[10]	0.420*[10]	50*[10]	NA		
	Collagen/ P(LLA-CL)		ES	46.6	20	NA	NA	4.0	1.77	4.912 mmHg*[15]	NA	HUSMCs	[160]
	Gelatin/Elastin/sodium hyaluronate		3D printing	NA	150	NA	400-500 μm*[16]	1.15	1.95*[17]	60	NA	NOF&NOK	[221]

*[1] solvent: trifluoroethanol (TFE), *[2] solvent: acetic acid and dimethylsulfoxide (DMSO), *[3] two different solvents (acetone and 1,1,1,3,3,3-Fluoro-2-propanol (HFIP)), *[4] resembles actual arteries, *[5] iCVD skin layer, *[6] PTFE supporting membrane, *[7] pore size of the PTFE membrane, *[8] longitudinal, *[9] across the fiber, *[10] taken from graphical depictions, *[11] no creep up to 15% strain at 0.25 Hz, *[12] PCL (MW 14,000), solvent: hexafluoro-2-propanol (HFP), *[13] PCL (MW 80,000), solvent: HFIP, *[14] preparation in two different flow rates, *[15] burst pressure, *[16] pore size of another side of the membrane is 50-150 μm, *[17] dynamic tensile storage modulus is 314 kPa

Polymeric membranes can play an important role in bioinspired lung cell models. Breathing-induced cyclic stretch is playing a pivotal role in lung biology. Current *in vitro* cell-stretching models can benefit from advanced membranes with tunable biophysical and mechanical properties. We offer perspectives on hybrid polymeric membranes mimicking the alveolar-capillary barrier.

Keyword: tunable polymeric membrane, porous ultra-thin scaffold, alveolar-capillary barrier, air-liquid interface cell culture*, in vitro* cell-stretching model,

Ali Doryab received his B.Sc. (2011) in Materials Engineering at Tehran Polytechnic and continued to pursue his M.S. (2013) in Biomedical Engineering at University of Tehran. He is currently a Ph.D. student at Helmholtz Zentrum München and Faculty of Medicine, Ludwig-Maximilians-University (LMU) of Munich under supervision of Dr. Otmar Schmid. His current research focuses on the next generation biomimetic bioreactor for the lung with cyclic mechanical stretch. His research interests include synthesis polymeric BioMembrane for lung and studying the physiology of mechanically stretched pulmonary cells.

Dr. Darcy Wagner is an Assistant Professor in the Faculty of Medicine at Lund University and she is the head of the Lung Bioengineering and Regeneration Group. She is a Principal Investigator in the Lund Wallenberg Molecular Medicine Center as well as the Lund Stem Cell Center. Her lab

focuses on generation of lung tissue *ex vivo* for eventual transplantation and building new humanized models of lung tissue to study chronic diseases and evaluate potential therapies. Her group takes a multidisciplinary approach using advances in materials science, manufacturing, and lung stem cell biology to construct these new models.

Dr. Otmar Schmid* (Corresponding Author) is head of the Pulmonary Aerosol Delivery Group at the Helmholtz Zentrum München and the Comprehensive Pneumology Center in Munich, Germany. He is also Adjunct Assistant Professor at the Missouri University of Science and Technology (USA). He is a physicist with more than 20 years of experience in aerosol science, inhalation toxicology and pulmonary drug delivery. He has developed advanced methods for aerosol delivery to preclinical in vitro and in vivo models of the lung including the patented ALICE-CLOUD technology. He has also worked lung imaging and on in vitro cell models and bioreactors of the lung.

Evolution of Bioengineered Lung Models: Recent Advances and Challenges in Tissue Mimicry for Studying the Role of Mechanical Forces in Cell Biology